

AFRL-ML-WP-TR-2000-4072

**HIGH THERMAL CONDUCTIVITY  
THERMOSETS FOR COMPOSITE  
APPLICATIONS**



**DR. GEORGE GOULD  
DR. KANG LEE**

**ASPEN SYSTEMS, INC.  
184 CEDAR HILL STREET  
MARLBOROUGH, MA 01752**

**MAY 2000**

**FINAL REPORT FOR 09/15/1997 – 03/15/2000**

**APPROVED FOR PUBLIC RELEASE; DISTRIBUTION UNLIMITED**

**MATERIALS AND MANUFACTURING DIRECTORATE  
AIR FORCE RESEARCH LABORATORY  
AIR FORCE MATERIEL COMMAND  
WRIGHT-PATTERSON AIR FORCE BASE OH 45433-7750**

**DTIC QUALITY INSPECTED 4**

**20000622 127**

## NOTICE

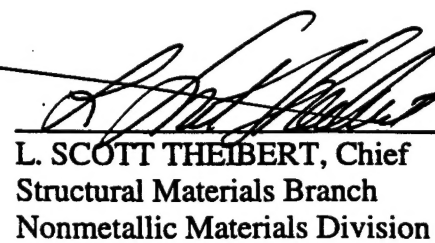
*Using Government drawings, specifications, or other data included in this document for any purpose other than Government procurement does not in any way obligate the U.S. Government. The fact that the Government formulated or supplied the drawings, specifications, or other data does not license the holder or any other person or corporation; or convey any rights or permission to manufacture, use, or sell any patented invention that may relate to them.*

*This report is releasable to the National Technical Information Service (NTIS). At NTIS, it will be available to the general public, including foreign nations.*

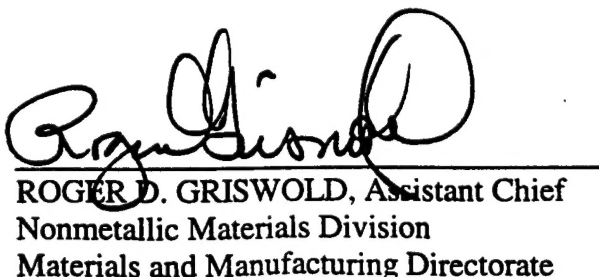
**THIS TECHNICAL REPORT HAS BEEN REVIEWED AND IS APPROVED FOR PUBLICATION.**



ROGER H. GERZESKI, Materials Engineer  
Composites Team  
Structural Materials Branch



L. SCOTT THEIBERT, Chief  
Structural Materials Branch  
Nonmetallic Materials Division



ROGER D. GRISWOLD, Assistant Chief  
Nonmetallic Materials Division  
Materials and Manufacturing Directorate

*Do not return copies of this report unless contractual obligations or notice on a specific document requires its return.*

## REPORT DOCUMENTATION PAGE

Form Approved  
OMB No. 0704-0188

Public reporting burden for this collection of information is estimated to average 1 hour per response, including the time for reviewing instructions, searching existing data sources, gathering and maintaining the data needed, and completing and reviewing the collection of information. Send comments regarding this burden estimate or any other aspect of this collection of information, including suggestions for reducing this burden, to Washington Headquarters Services, Directorate for Information Operations and Reports, 1215 Jefferson Davis Highway, Suite 1204, Arlington, VA 22202-4302, and to the Office of Management and Budget, Paperwork Reduction Project (0704-0188), Washington, DC 20503.

1. AGENCY USE ONLY (Leave blank)	2. REPORT DATE	3. REPORT TYPE AND DATES COVERED	
	MAY 2000	FINAL REPORT FOR 09/15/1997 - 03/15/2000	
4. TITLE AND SUBTITLE HIGH THERMAL CONDUCTIVITY THERMOSETS FOR COMPOSITE APPLICATIONS			5. FUNDING NUMBERS C F33615-97-C-5012 PE 62102 PR 4347 TA 36 WU 06
6. AUTHOR(S) DR. GEORGE GOULD DR. KANG LEE			
7. PERFORMING ORGANIZATION NAME(S) AND ADDRESS(ES) ASPEN SYSTEMS, INC. 184 CEDAR HILL STREET MARLBOROUGH, MA 01752			8. PERFORMING ORGANIZATION REPORT NUMBER
9. SPONSORING/MONITORING AGENCY NAME(S) AND ADDRESS(ES) MATERIALS AND MANUFACTURING DIRECTORATE AIR FORCE RESEARCH LABORATORY AIR FORCE MATERIEL COMMAND WRIGHT-PATTERSON AFB, OH 45433-7750 POC: ROGER GERZESKI, AFRL/MLBC, 937-255-9058			10. SPONSORING/MONITORING AGENCY REPORT NUMBER AFRL-ML-WP-TR-2000-4072
11. SUPPLEMENTARY NOTES			
12a. DISTRIBUTION AVAILABILITY STATEMENT APPROVED FOR PUBLIC RELEASE, DISTRIBUTION UNLIMITED.		12b. DISTRIBUTION CODE	
13. ABSTRACT (Maximum 200 words) A new class of discotic liquid crystal (DLC) epoxy resins have been developed which show a marginal degree of enhanced thermal transport properties compared to conventional, amorphous epoxy resins. The DLCs feature metallocenesogen cores with various pendant flexible spacer groups, can be cured individually or as blends of different types of DLCs with a variety of aliphatic and aromatic polyamines at low temperatures (80 to 100 C) to give strong, semi-flexible films. The Z axis thermal conductivity values for these novel cured DLCs range between 0.24 and 0.30 W/m-K as compared to roughly 0.20 W/m-K for conventional epoxy resins.			
14. SUBJECT TERMS Thermally Conductive Polymers, Composites, Electronic Packaging, Thermal Management		15. NUMBER OF PAGES 80	
		16. PRICE CODE	
17. SECURITY CLASSIFICATION OF REPORT UNCLASSIFIED	18. SECURITY CLASSIFICATION OF THIS PAGE UNCLASSIFIED	19. SECURITY CLASSIFICATION OF ABSTRACT UNCLASSIFIED	20. LIMITATION OF ABSTRACT SAR

## Table Of Contents

	Table Of Contents	iii
	List Of Figures	iv
	List Of Tables	vii
	Executive Summary	viii
1	Introduction	1
1.1	Thermally Conductive Polymer Matrices	1
1.2	Liquid Crystal Mesophases	2
1.3	Discotic Mesophases	4
1.4	Cross-Linking Reactions	5
1.5	The Effects of Filler Materials	6
1.6	Thermal Conductivity in Solids	7
2	Experimental Procedures	11
2.1	Synthesis of Discotic Liquid Crystalline Monomers	11
2.2	Synthesis of Discotic Liquid Crystalline Metallociketonate Monomers	19
2.3	Cu(II) carboxylate metallomesogens	38
2.4	Discotic LC resin curing chemistry	55
2.5	Summary of synthesis, isolation and curing of discotic LC thermoset resins	65
3.1.	Thermal conductivity Testing Methods	66
3.2	Thermal conductivity results for cured discotic LC resins	67
3.3.	Summary of thermal conductivity results for cured discotic LC resins	69
4.	References	69

## List Of Figures

Figure 1. Z-directional molecular ordering in discotic LC (monomers enlarged for illustration)

Figure 2. Molecular states of rod-like mesogens,  $n^\rightarrow$  denotes orientational order director

Figure 3. Nematic Discotic ( $N_D$ ) Phase

Figure 4. Columnar phases of disc shaped molecules a) hexagonal ordered; b) hexagonal ordered top view; c) hexagonal disordered; d) rectangular (top view; ellipses denote tilted disks with respect to column axis); e) tilted.

Figure 5. Schematic of a discotic liquid crystal epoxy resin. Each disk represents a metallomesogenic core functionalized with multiple alkyl groups of variable length.

Figure 6. Liquid Crystalline Configuration of Aspens' Monomers and Resulting Polymer.

Figure 7. Idealized smectic phase of a mesogenic monomer showing a high functional group density.

Figure 8. Detail of complete cross-linking reaction of epoxy groups with 1,4-diaminobenzene from within a dense discotic LC mesophase structure (a metallophthalocyanine derivative is shown).

Figure 9. Schematic description of the proposed composite material of liquid crystal epoxy resin and thermally conductive filler. The LC epoxy matrix between fillers will 1) *form thermally conductive crystal domains*, 2) *provide a thermal conduction array*, and 3) *reduce boundary thermal resistance at the filler-polymer interfaces*.

Figure 10. Thermal conductivity of polymer-based composites

Figure 11. Structure of Phthalocyanine Metal Complex with Side Chains

Figure 12. Synthetic pathway for the epoxy functionalized discotic Pc monomer

Figure 13. Synthesis and purification of 1,2-dicyano-4,5-dimethoxybenzene

Figure 14. Purification of 1,2-dicyano-4,5-dimethoxybenzene liquid crystalline and isotropic phases in the alcohol substituted material.

Figure 15. First heating DSC of  $CuPc[O(CH_2)_{12}OH]_8$ :

Figure 16. Second heating scan of  $CuPc[O(CH_2)_{12}OH]_8$ .

Figure 18. General synthetic approach to a discotic  $\beta$ -diketonate complex with epoxy modified pendant alkyl chains.

Figure 19. Epichlorohydrin route for the synthesis of di-ketone ligand with pendant epoxy groups.

Figure 20. Peroxidation method for the synthesis of the di-ketone ligand with pendant epoxy groups.

Figure 21. 1-(3'4'-dimethoxyphenyl)-3-(3",4",5"-trimethoxyphenyl)propane-1,3-dione preparation

Figure 22. Bis[1-(3'4'-dimethoxyphenyl)-3-(3",4",5"-trimethoxyphenyl)propane-1,3-dioato] copper(II) complex preparation

Figure 23. The structure of 1-(3'4'-dihydroxyundecanoxyphenyl)-3-(3",4",5"-trihydroxyundecanoxyphenyl) propane-1,3-dione

Figure 24. First heating DSC thermogram of bis[1-(3',4'-dihydroxyundecanoxyphenyl)-3-(3",4",5"-trihydroxyundecanoxyphenyl)propane-1,3-dionato]copper(II). Heating rate was 10°C/min.

Figure 25. Second heating DSC of bis[1-(3',4'-dihydroxyundecanoxyphenyl)-3-(3",4",5"-trihydroxyundecanoxyphenyl)propane-1,3-dionato]copper(II). Heating rate 10 °C/min.

Figure 26. Epoxidation of 1-(3',4'-dihydroxyundecanoxyphenyl)-3-(3",4",5"-trihydroxyundecanoxyphenyl) propane-1,3-dione with epichlorohydrin and  $NaAlO_2$ .

Figure 27. Acryloylation of the pentaalcohol  $\beta$ -diketone core.

Figure 28. Reaction sequence for alkylating the pentaphenol mesogen core with an  $\alpha,\omega$ -bromoalkene and subsequent conversion to the pentaepoxide.

Figure 29. Square planar, bis-ligand Cu(II) complex of the fully epoxidized  $\beta$ -diketonate monomer. This material does not show any liquid crystalline phases.

Figure 30. Synthesis and purification of long chain pentaalkene modified  $\beta$ -diketone.

Figure 31. Synthesis and isolation pathway for the  $\beta$ -diketone core with  $-O-(CH_2)_9OH$  substitutions.

Figure 32. Next generation design for discotic LC thermoset monomers.

Figure 33. Synthetic pathway to the 8-arm epoxy substituted discotic LC thermoset based on Cu(II) coordinated substituted carboxylates.

Figure 34. Synthetic pathway to the 8-arm acrylate substituted discotic LC thermoset based on Cu(II) coordinated substituted carboxylates.

Figure 35. Idealized structure of the  $Cu_2(OCOR)_4$  discotic LC thermosets.

List Of Figures Continued

Figure 36. Synthesis of methyl 3,5-bis(11-hydroxyundecanoxy) benzoate  
Figure 37. Synthesis of 3,5-bis(11-hydroxyundecanoxy) benzoic acid  
Figure 38. Structure of the dicopper complex of 3,5-bis(11-hydroxy-undecanoxy) benzoate.  
Figure 39. First DSC heating and cooling thermograms for of the dicopper complex of 3,5-bis(11-hydroxy-undecanoxy)benzoate  
Figure 40. Birefringence behavior of the dicopper complex of 3,5-bis(11-hydroxyundecanoxy)benzoate at 140 °C (under crossed polarization).  
Figure 41. Birefringence behavior of the same dicopper complex of 3,5-bis(11-hydroxyundecanoxy)benzoate at 160 °C (under crossed polarization).  
Figure 42. Synthesis of 3,5-bis(11-acryloyloxyundecanoxy) benzoic acid  
Figure 43. Structure of the Cu(II) complex of 3,5-bis(11-acryloylundecanoxy) benzoate.  
Figure 44. DSC analysis of the Cu(II) complex of 3,5-bis(11-acryloyl-undecanoxy)benzoate.  
Figure 45. Hot stage microscope birefringence behavior of a thin film sample of the Cu(II) complex of 3,5-bis(11-acryloylundecanoxy) benzoate at different temperatures. Polarized transmitted light was used to illuminate the sample and a polarizer oriented perpendicular to the plane of the polarized transmitted light was placed on top of the sample. Temperatures for each view: (a) 40 °C, (b) 50 °C, (c) 55 °C, (d) 60 °C, (e) 65 °C  
Figure 46. Synthesis of 3,5-bis(11-dodecenoxy)benzoic acid  
Figure 47. Synthetic procedure for epoxidation of the benzoic acid ligand with a n=10 flexible chain length.  
Figure 48. The structure of the prepared discotic LC epoxy.  
Figure 49. Birefringence images of discotic LC epoxy resin  
Figure 50. First DSC heating thermogram of the n=9 discotic LC epoxy complex. Heating rate: 10 °C.  
Figure 51. Synthetic pathway to a new discotic LC monomer with higher transition temperature  
Figure 52. Preparation of 6-bromo-1-hexene for use in synthesizing discotic LC epoxy resins with shorter flexible spacers (for raising LC transition temperatures).  
Figure 53. Synthetic pathway to the short flexible spacer (n=4) 8-arm discotic LC epoxy monomer.  
Figure 54. Structure of the discotic LC epoxy monomer with shorter flexible spacer arms (n=4) intended to give a higher LC transition temperature compared to the previous longer chained resins.  
Figure 55. DSC thermogram for n=4, 8-arm discotic LC epoxy monomer. The peak at 94 °C is assigned to the crystalline to discotic phase transition ( $K \rightarrow N_d$ ) and the larger endothermic peak at 141 °C is assigned to the discotic to isotropic melting transition ( $N_d \rightarrow I$ ).  
Figure 56. Polarized optical microscopy of the n=4, 8-arm discotic LC epoxy resin.  
Figure 57. After free radical curing above the isotropic clearing temperature, the discotic LC acrylate (n=11) thermoset resin still shows crystalline order.  
Figure 58. Solvent casting method used to make thin thermoset polymer films from discotic LC epoxy resins and polyfunctional amine curing agents.  
Figure 59. Discotic LC epoxy monomer (n=4) mixed with diethylenetriamine in THF at room temperature.  
Figure 60. Polyamines used for discotic LC epoxy curing  
Figure 61. Structure of the discotic liquid crystal epoxy thermoset monomer (n=9).  
Figure 62. Synthetic procedure (modified) for the synthesis of the improved 4-arm, n=9 discotic LC epoxy resin.  
Figure 63. DSC thermogram of 4-armed, n=9 discotic LC epoxy.  
Figure 64. Cross-polarized microscopic view of film from 4-arm, n=9 discotic LC epoxy monomer cured with 1,3-diaminopropane at room temperature.  
Figure 65. LC phase observed in film of 80% 4-arm monomer and 20% 8-arm monomer cured with 1,3-propanediamine at room temperature (1 week) followed by a post-cure anneal at 100 °C (3 hours).  
Figure 66. Birefringence images of 4-arm/8-arm discotic blending systems (a) after room temperature curing and (b) after 50°C curing.  
Figure 67. Synthetic pathway to the aliphatic discotic epoxy co-monomer  
Figure 68. (a) Sample 1 and (b) sample 2 from Table 7 above. The films were cured for four days at room temperature when these birefringence images were taken.

List Of Figures Continued

Figure 69. DHAMS, the diglycidyl ether of dihydroxy- $\alpha$ -methylstilbene

Figure 70. Birefringence image of a film of DHAMS cured with DADS in the smectic LC state.

## List Of Tables

Table 1. New Thermoset monomers with discotic LC characteristics based on metallomesogens.  
Table 2. Fabrication of samples with discotic liquid crystal epoxy (n=4).  
Table 3. Fabrication of samples with discotic liquid crystal epoxy (n=9).  
Table 4. Discotic liquid crystal epoxy thermoset (4-arm, n=9) curing amines.  
Table 5. Discotic liquid crystal epoxy mixtures cured with 1,3-diaminopropane at room temp.  
Table 6. Aliphatic discotic epoxy blends with 4-arm (n=9) discotic LC epoxy cured with 1,3-propanediamine at room temperature.  
Table 7. Thermal conductivity results for the 8-arm, discotic LC epoxies with n=4 and n=9 flexible spacer chain lengths cured with 1,3-propanediamine.  
Table 8. Summary of laser flash thermal conductivity results for the best candidate discotic LC epoxy films cured with 1,3-propanediamine.

## Executive Summary

### Introduction:

Thermally conductive materials are important components of aerospace structures where heat must be rapidly dissipated from components. Metals such as aluminum have traditionally filled this role, but the need to reduce weight has driven the search for lighter thermally conductive materials. While polymer matrix composite structures have become attractive light weight replacements for metals in many structural applications, the very low thermal conductivity (TC) of organic polymers has severely limited their application in materials where heat dissipation is required.

Aspen system proposed a conceptually new approach to polymer matrices with inherently high TC. These materials are based on discotic liquid crystal (DLC) thermoset materials that spontaneously align into highly ordered columnar structures. Modification of these DLCs with epoxy groups leads to cross-linking of the aligned structures with appropriate curing agents, freezing in the alignment and resulting in cured thermosets with a higher degree of Z-directional molecular order. This order was envisioned as a way to promote the transfer of thermal energy through the material. This would ideally result in a composite material with higher TC in the Z direction.

### Program Goals And Technical Approach:

The goals of this research project were: i. develop synthetic routes to a series of epoxy modified DLC monomers, ii. demonstrate monomer curing via cross-linking agents, while retaining Z-directional orientation, iii. assess physical properties of thermally conductive polymer matrices, iv. test TC of the cured materials.

### Results And Accomplishments:

Of the candidate DLC resins, the benzoate systems have the most promise based on synthetic economy and physical performance. Numerous processing conditions yielded cross-linked matrices which retained the LC character in the Copper mesogenic based resins. Using the procedures described, these resins would still be too costly, when compared to commodity resins, for large scale applications.

#### Conclusions And Recommendations:

TC results obtained for these DLC resins were disappointing. They were only nominally better than standard resin matrices. The relatively difficult and expensive to synthesize epoxy DLC resins which were the focus of this research project DO NOT enhance TC in the Z direction substantially as compared to more easily obtainable rod like LC epoxy resins, and only moderately better than conventional bis-phenol A epoxy resin. A more processable version of the rod like LC resin, one that would allow for a much lower curing temperature and higher solubility may allow for higher TC resins to be economically manufactured.

## 1 Introduction

### 1.1 Thermally Conductive Polymer Matrices

Thermally conductive materials are important components of aerospace structures where heat must be rapidly dissipated from electrical or mechanical components. Light weight metals such as aluminum have traditionally filled this role, but increasing pressure to reduce payload weight has driven the search for even lighter thermally conductive materials. While polymer matrix composite structures have become attractive light weight replacements for metals in many structural applications, the very low thermal conductivity of organic polymers has severely limited their application in materials where heat dissipation is required.

A number of modifications to organic polymer matrix composites have been developed to increase their thermal conductivity. The use of highly conductive fibers such as graphite in the composite results in dramatic increases in thermal conductivity, since the fibers act as conduits for the thermal energy. Unfortunately, the laminar orientation of the fibers within the composite essentially limits the thermal conductivity to the X and Y directions within the material, and the Z direction thermal conductivity is negligible. To address this concern, “z-stitched” materials have been developed in which fibers are woven into the composite structure so that they are oriented normal to the fiber orientation. Unfortunately, z-stitching requires expensive additional equipment in the manufacturing process, and the stitching process frequently damages the structural integrity of the composite fibers.

To address these challenges, Aspen Systems proposed a conceptually new approach to organic polymer matrices with inherently high thermal conductivity. These materials

are based on discotic liquid crystalline (LC) thermoset materials that spontaneously align into highly ordered molecular structures with columnar orientation. Modification of these LC materials with epoxy groups leads to cross-linking of the aligned structures in the presence of appropriate curing agents, thus “freezing” the molecular order into the thermoset and resulting in cured solids with a higher degree of Z-directional molecular order. The tight packing of the monomers in columnar stacks between the composite fibers, as shown in Figure 1, was envisioned to promote the transfer of thermal energy through the material. This would ideally result in a composite material with inherently high thermal conductivity in the Z direction.

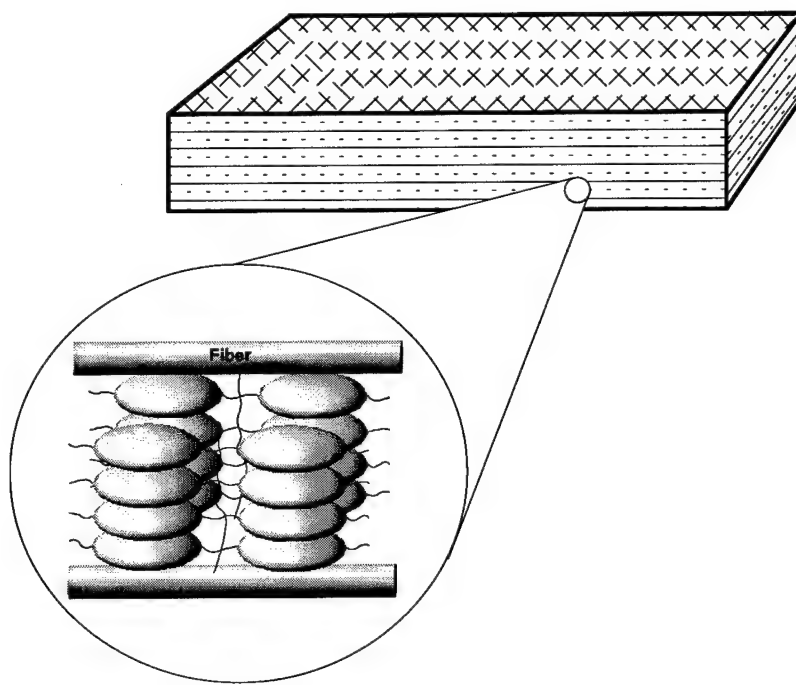


Figure 1. Z-directional molecular ordering in discotic LC (monomers enlarged for illustration)

## 1.2 Liquid Crystal Mesophases

The liquid crystal (LC) state, or mesophase, is a distinct phase of matter observed between the crystalline (solid) and isotropic (liquid) states. In the LC state, the molecules retain some of their orientational order and some of their positional order from the solid

state, as a result of thermodynamically driven molecular self alignment. The specific molecular structure dictates whether or not a material exhibits liquid crystallinity and what type of mesophase it displays. In this program we are concerned with thermotropic liquid crystals, defined by the fact that the transitions to the liquid crystalline state are induced thermally. One can arrive at the liquid crystalline state by raising the temperature of a solid and/or lowering the temperature of a liquid. In general, thermotropic mesophases occur because of anisotropic dispersion forces between the molecules and enhanced packing interactions. These forces, derived from specific intermolecular interactions, dictate the type of thermotropic phase exhibited.

Figure 2 illustrates the smectic and nematic phases of the classical rod-like mesogenic systems;  $n^{\rightarrow}$  denotes the orientational order director, or the preferential direction of alignment. Rod-like idealized smectic thermotropes arrange themselves in a lamellar structure with all of the molecules lying parallel to each other in two or three dimensions, retaining a long range of positional and orientational order. In the nematic phase, also shown in Figure 2, rod-like molecules align in a thread-like fashion, retaining a long range of orientational order, while losing their long range positional order. A standard isotropic resin system, in contrast, has no long range order, and consists of masses of entangled molecules in random orientation.

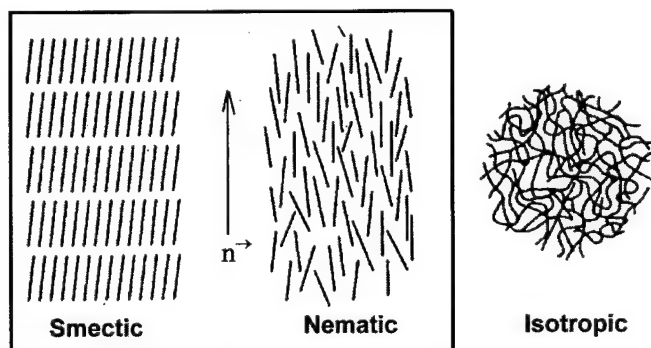


Figure 2. Molecular states of rod-like mesogens,  $n^{\rightarrow}$  denotes orientational order director

### 1.3 Discotic Mesophases

Thermotropic mesophases are also found in molecules of disc-like shape, and are often labeled as “discotic”. Similar to the rod-like molecules, discotic mesophatic molecules form a nematic phase characterized by long range orientational order, but no long range positional order. The director,  $n^{\rightarrow}$ , now denotes the preferred direction of the discs, shown schematically in Figure 3. In most cases, however, the disc-shaped molecules are packed one upon another to form columns with varying degrees of order, shown schematically in Figure 4.

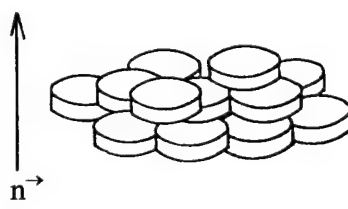


Figure 3. Nematic Discotic (N<sub>D</sub>) phase.

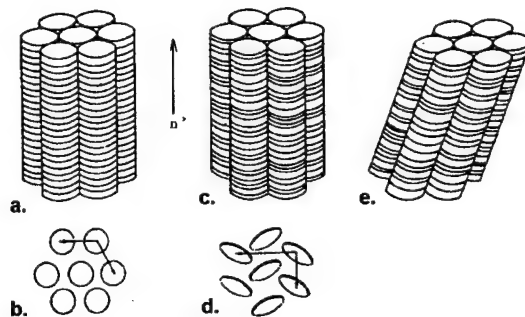


Figure 4. Columnar phases of disc shaped molecules a) hexagonal ordered; b) hexagonal ordered top view; c) hexagonal disordered; d) rectangular (top view; ellipses denote tilted disks with respect to column axis); e) tilted.

Three different classes of discotic mesophases have been defined: nematic, columnar and lamellar.<sup>1</sup> A typical discotic compound consists of flat, rigid cores which are surrounded by flexible chains. The effect of the chains is to lower the phase transition of the LC (crystalline to discotic transition), and to isolate the columns from one to another so that the structure has some mobility.<sup>2</sup> Figure 5 shows a schematic of a hexagonally ordered discotic phase. In addition to the hexagonal phase shown in Figure 5, rectangular and tetragonal discotic phases have also been described in the literature.<sup>1</sup>

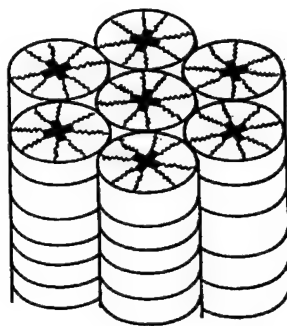


Figure 5. Schematic of a discotic liquid crystal epoxy resin. Each disk represents a metallomesogenic core functionalized with multiple alkyl groups of variable length.

#### 1.4 Cross-Linking Reactions

Previous work at Aspen Systems in the area of rigid rod liquid crystalline thermosets has illustrated that an LC epoxy monomer phase can be successfully cross-linked by amine co-reactants to give a cured epoxy resin that retains its three-dimensional order at the molecular level, as indicated by strong birefringence in the solid.<sup>3</sup> Aspen Systems developed an approach to a new class of materials designed to overcome the cost and damage tolerance issues associated with resins processed at high temperatures.<sup>3</sup> By placing the reactive groups at the end of orderable liquid crystalline segments as shown in Figure 6, the reactive groups are maintained adjacent to each other, and are therefore concentrated into a small fraction of the materials molecular volume as shown in Figure 7. Because of the close proximity of the reactive groups, little or no molecular motion is needed for group interaction and complete conversion is no longer a function of molecular diffusion within the bulk system (this is particularly true of homopolymerization reactions). High polymer conversion was observed well below the final polymer  $T_g$  using aromatic diamine curing agents. Flexible aliphatic alkyl chain spacer groups positioned between the oxirane functional groups and the aromatic mesogen core

act as a plasticizer. This plastic deformation zone was designed to dissipate fracture energy and thus reduce crack propagation in laminated composites. Unfortunately, this plasticity also significantly lowers the  $T_g$  of the resulting polymer.

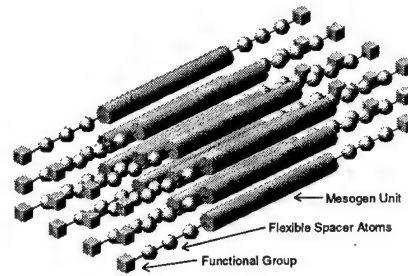
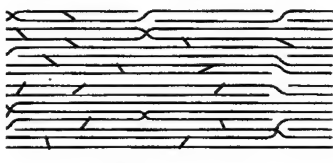


Figure 6. Liquid Crystalline Configuration of Aspens' Monomers and Resulting Polymer.

Figure 7. Idealized smectic phase of a mesogenic monomer showing a high functional group density.

Epoxy matrices offer high thermal stability and chemical resistance, and are currently used in numerous composite materials as matrix resins. Small, nucleophilic diamine co-reactants can be employed as cross-linking reagents for the epoxy groups in order to minimize disruption of the LC discotic mesophase. Heating of the epoxy/diamine mixture in the discotic fluid results in reaction between the amine group and the epoxy to give cross-linking between the stacked discotic monomers as well as between adjacent columns in the discotic mesophase. Consequently, the discotic matrix is completely immobilized in the columnar orientation. Figure 8 illustrates a cross-linking reaction between an epoxy functionalized metal phthalocyanine and 1,4-diaminobenzene.

### 1.5 The Effects of Filler Materials

The polymer matrices developed in this program are based on discotic liquid crystalline (LC) thermoset materials that spontaneously align into highly ordered molecular structures with columnar orientation. Modification of these LC materials with epoxy groups allows cross-linking of the aligned structures upon reaction with difunctional amine reagents, freezing the molecular order into the thermoset. The

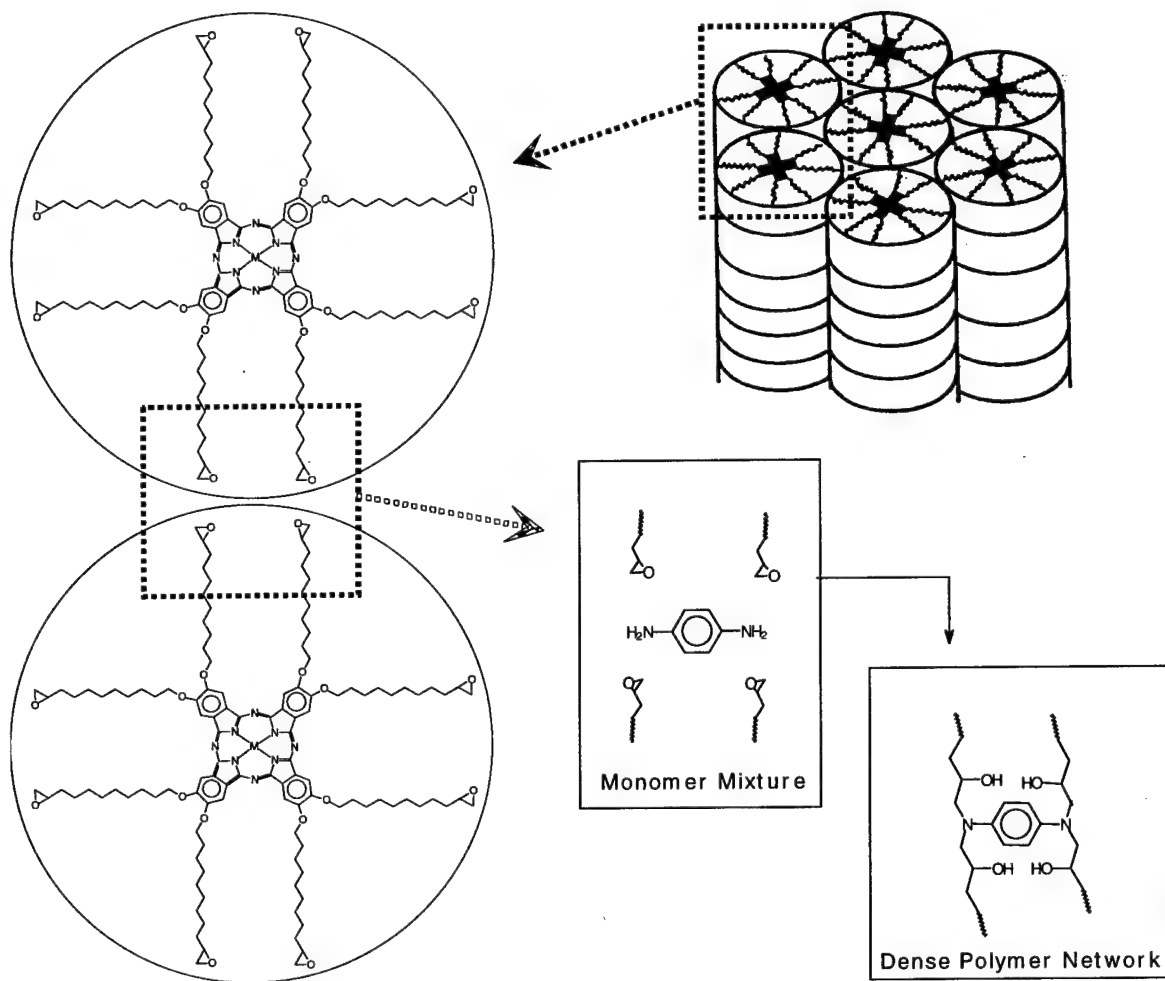


Figure 8. Detail of complete cross-linking reaction of epoxy groups with 1,4-diaminobenzene from within a dense discotic LC mesophase structure (a metallophthalocyanine derivative is shown).

resulting cured solids will have a high degree of molecular order provided the materials were in a liquid crystalline phase during the curing cycle. The tight packing of the monomers in columnar stacks between fibers (Figure 1) or ceramic filler particles (Figure 9) promotes the transfer of thermal energy through the material and results in a composite material with higher thermal conductivity.

### 1.6 Thermal Conductivity in Solids

In order to develop organic composite materials with improved thermal conductivity, the origins of conductivity in a solid material must be understood. Thermal conductivity

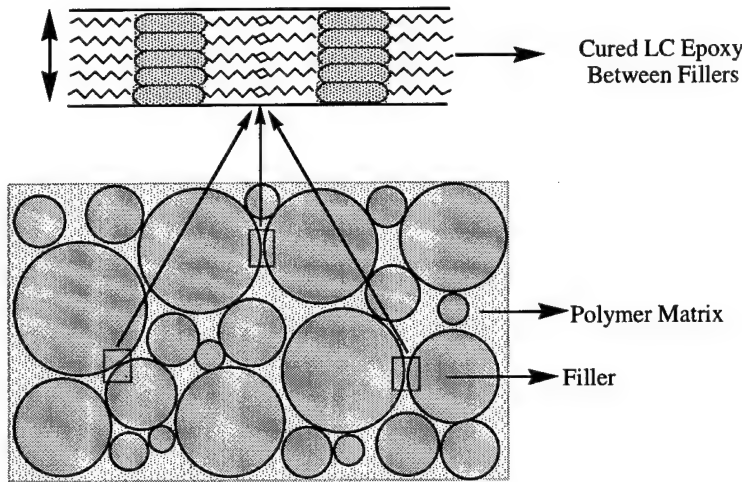


Figure 9. Schematic description of the proposed composite material of liquid crystal epoxy resin and thermally conductive filler. The LC epoxy matrix between fillers will 1) *form thermally conductive crystal domains*, 2) *provide a thermal conduction array*, and 3) *reduce boundary thermal resistance at the filler-polymer interfaces*.

( $k$ ) is the rate of heat flow through a material and is determined primarily by three factors: (i) the amount of heat energy present, (ii) the nature of the heat carrier in the material, and (iii) the amount of heat dissipation. The heat energy present in a material is a function of the heat capacity  $c$ . The heat carriers are either electrons or quantized lattice vibrations known as phonons. The amount of heat dissipation is a function of scattering effects and can be considered as the mean free path of the lattice vibration. If the quantity and velocity of the carrier is  $v$  and the mean free path is  $l$ , then  $k$  can be expressed by the following equation:

$$k \sim cvl \quad (1)$$

Consequently, thermal conductivity in a solid can be increased by increasing the heat capacity, increasing the number and velocity of the carriers, or by increasing the mean free path, equivalent to decreasing the scattering of the vibrations.

The thermal conductivity of polymer-ceramic composite materials is a function of the thermal conductivities of polymer matrix, polymer – filler interface, and filler, as shown

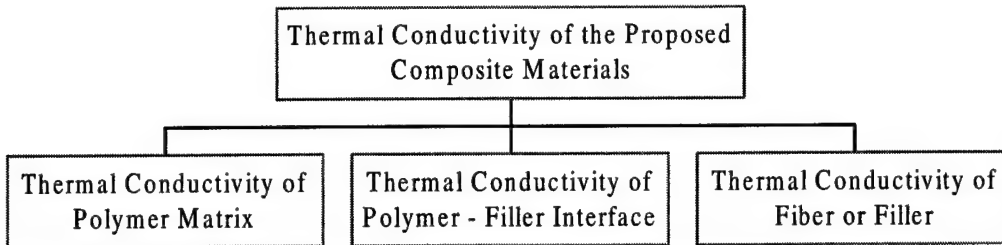


Figure 10. Thermal conductivity of polymer-based composites

in Figure 10. Theoretical predictions of thermal conductivity of polymer – ceramic composites have been well documented in the literature.<sup>4-8</sup> In general, the following parameters must be addressed when developing a thermally conductive polymer – ceramic composite:

1) Effect of the Filler. Higher thermal conductivity filler results in a composite with higher thermal conductivity. However, as discussed by Bigg,<sup>6</sup> when the intrinsic thermal conductivity of the filler is 100 times greater than that of the polymer matrix, there is no significant improvement in the composite thermal conductivity. This observation has been made in a number of epoxy – ceramic composite systems.<sup>9</sup> On the other hand, the maximum filler loading is restricted to 60% to 70% volume fraction range theoretically. Due to these limitations, the opportunity for innovation appears to lie exclusively in thermal conductivity improvements made to the polymer matrix and polymer-filler interface.

2) Thermal Conductivity of the Polymer. Most organic polymers have low thermal conductivity because of the large molecular size, the lack of crystallinity and the random orientation of covalent bonds that allow rapid dissipation of the phonons and shorten the mean free path. Typical thermal conductivity values for common organic polymers fall in the range of 0.08 to 0.33 W/m K at room temperature.

However, the semicrystalline regions in the polymer have relatively higher thermal conductivity than the amorphous regions.<sup>10</sup> Shear alignment induced via drawing of a polymer partially aligns these crystalline domains, substantially increasing the bulk thermal conductivity.<sup>11</sup> Therefore, improved  $k$  values in polymeric materials are attainable if the molecules can be properly aligned. Discotic liquid crystalline materials provide thermodynamically driven self-alignment, enabling the development of thermoset matrices that retain a high degree of order.

3) Thermal Boundary Resistance ( $R_b$ ) at Polymer-Filler Interface. The thermal conductivity of composites made from amorphous epoxy resin has been successfully explained on the basis of a two-phase model which incorporates thermal boundary resistance.<sup>12</sup> This model takes into account all the relevant factors: the thermal conductivities of the filler and the matrix, the shape, size and concentration of the filler, and the boundary resistance  $R_b$ , which are all measurable quantities in the case of composite materials. The acoustic mismatch between filler and amorphous polymer matrix introduces an additional thermal resistance. This thermal boundary resistance  $R_b$  depends on the sound velocities and densities of the amorphous (polymer) and crystalline (filler) regions, respectively, and will be larger if there is greater disparity in these quantities in the two phases.

Based on the above discussion, high thermal conductivity in polymer-based composites is achievable if reasonably thermally conductive polymer resins are used as a matrix. The discotic liquid crystal epoxies developed during this project will tend to self-align on the filler surface and thus reduce the thermal boundary resistance ( $R_b$ ) at the polymer resin-filler interface. The liquid crystal phase of the discotic LC epoxy will be

retained after curing at the appropriate temperature. The column structure of the cured discotic LC epoxy will provide a thermal conduction pathway in the polymer matrix between filler particles.

According to Agari's theoretical thermal conductivity equation:

$$\log \lambda_c = V_f \times C_2 \times \log \lambda_f + (1-V_f) \times \log (C_1 \times \lambda_p) \quad (2)$$

(where  $\lambda_c$ ,  $\lambda_f$ , and  $\lambda_p$  are the thermal conductivity of composite, filler and polymer matrix respectively;  $V_f$  is the volume content of fillers;  $C_2$ , the coefficient of ease in forming conductive chains of fillers;  $C_1$ , the coefficient of the effect of crystallinity and crystal size of polymer), the proposed system will substantially increase both  $C_1$  and  $\lambda_p$ .

## 2 Experimental Procedures

### 2.1 Synthesis of Discotic Liquid Crystalline Monomers

Metal containing phthalocyanines (Pc) have been widely studied because of their high thermal stability, chemical resistance and interesting electronic properties arising from the transition metal ion and electron rich structure. Functionalized Pc's have been incorporated into a number of polymer systems including epoxies and polyimides resulting in materials with decomposition temperatures of over 500°C.<sup>13,14</sup> Unsubstituted Cu Pc can be sublimed under vacuum at 580°C without decomposition and is resistant to strong mineral acids. Despite considerable interest in Pc materials, however, the high temperature materials applications of these compounds have generally remained separate from work involving the liquid crystalline properties of the Pc's.

Modification of the Pc structure with eight alkyl side chains, as shown in Figure 11, has been found to result in discotic liquid crystalline materials by several researchers.<sup>15,16</sup> The favorable interaction between the aromatic pi-electron systems of

the adjacent molecules as well as the attractive forces between the alkyl side chains result in a thermodynamic preference for the molecules to form a vertically stacked array. The distances between the Cu ions in a vertically stacked array of Pc complexes was estimated to be 3.4 Å, a distance which was predicted to facilitate interactions between the Pc subunits including ferro- and antiferromagnetism, exciton transport and electron transfer conduction.

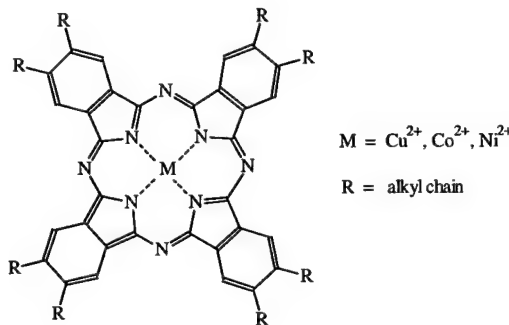


Figure 11. Structure of Phthalocyanine Metal Complex with Side Chains

In this project, we prepared an epoxy functionalized Pc ligand analogous to the structure shown in Figure 11 (and the corresponding Cu(II) complex). The synthesis of a prototypical epoxy functionalized discotic Pc monomer is illustrated in Figure 12. The preparation of the Pc core was based on well established literature procedures.<sup>17</sup> Reaction of the  $\text{Pc}-(\text{OH})_8$  core with a long chain bromoalcohol ( $n = 8-12$ ) resulted in hydroxy functionalized alkyl chains in the eight substitution positions around the core. Reaction of the hydroxy derivative with epichlorohydrin under basic conditions gives the epoxy functionalized product as shown.

The detailed synthetic procedures to get to the epoxy functionalized Pc monomer are provided below.

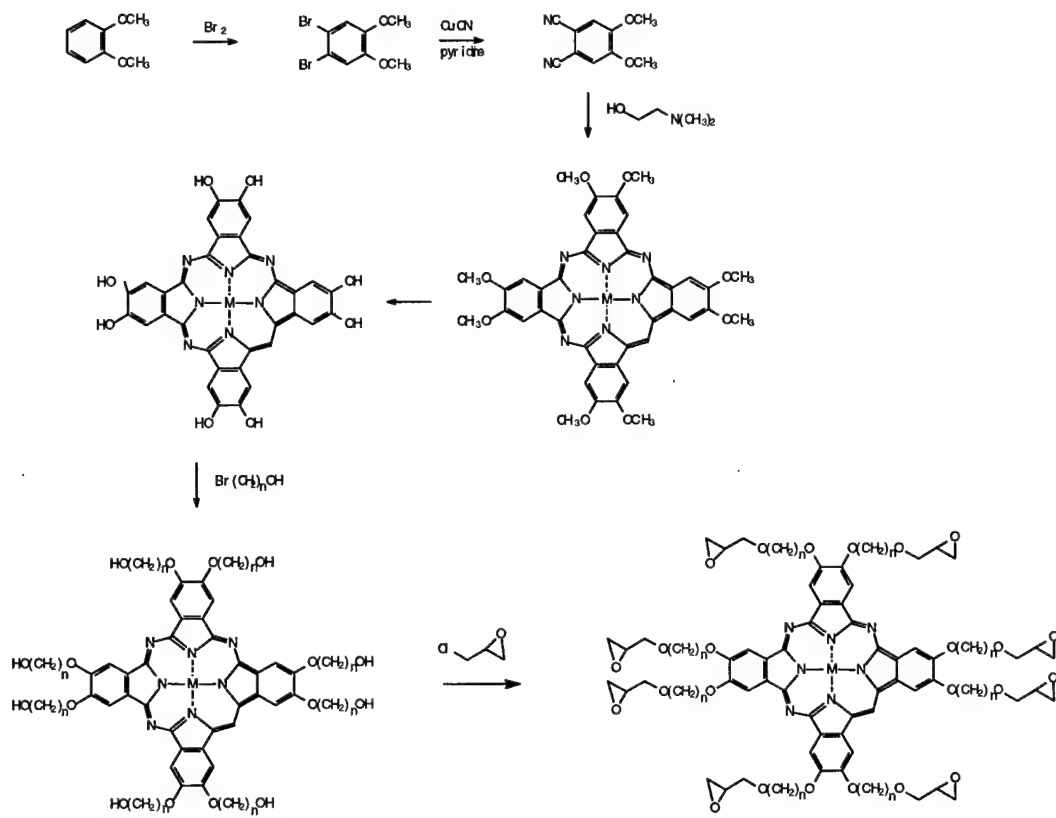


Figure 12. Synthetic pathway for the epoxy functionalized discotic Pc monomer

### 2.1.1. Preparation of 1,2-dibromo-4,5-dimethoxybenzene:

The title compound has been synthesized by the literature procedure.<sup>17</sup> In a 1 L round-bottomed flask, 138 grams (1 mole) veratrole (1,2-dimethoxybenzene) and 400 mL acetic acid were added. The flask was then placed in a 0°C ice-bath. 320 grams (2 mol) of Br<sub>2</sub> dissolved in 250 mL acetic acid was added through an addition funnel for a period of 1 to 1.5 hours. The reaction was continued for another one hour with magnetic stirring at 0°C. After the reaction, the suspension was diluted with about 1.5 liter of H<sub>2</sub>O, the solid residue which was separated by filtration was washed with 1 liter of 5% NaOH solution and finally with water for several times to pH ~ 7 and dried in vacuum oven. The crude product is powder with slightly yellow color.

The crude product was dissolved in about 500 mL chloroform, 750 mL ethanol was then added and the 1,2-dibromo-4,5-dimethoxybenzene was crystallized at room temperature. The crystal was separated by filtration and dried in vacuum oven (Fraction **1**, 110 grams). The product in the solution can be further crystallized by keeping the temperature at 0°C (Fraction **2**, 72 grams). After filtration, the solution was condensed by rotoevaporator and a small amount of ethanol was added and thus recover the most product in solution (Fraction **3**, 76 grams). Total yield: 258 grams, 87 % of theory (254 grams, 86% in literature); colorless needle-like crystal.

All of the 3 fractions during the purification have the identical melting point (84 ~ 86°C).  $^1\text{H-NMR}$  result (see Figure 1) confirmed that the product had the expected structure.  $^1\text{H-NMR}$  (Figure **1**, in  $\text{CDCl}_3$ ):  $\delta$  3.88 ppm (s, 6H,  $-\text{CH}_3$ ),  $\delta$  7.09 ppm(s, 2H, ArH). Literature data<sup>17</sup>:  $^1\text{H-NMR}$  ( $\text{CDCl}_3$ ):  $\delta$  3.85 ppm (s, 6H,  $-\text{CH}_3$ ),  $\delta$  7.05 ppm(s, 2H, ArH).

#### 2.1.2. Preparation of 1,2-dicyano-4,5-dimethoxybenzene:

1,2-Dibromo-4,5-dimethoxybenzene (44.4 grams, 0.15 mol), CuCN (40.3 grams, 0.45 mol) and 600 mL DMF were heated and refluxed in a 1 liter round-bottomed flask for 5 hours. After being cooled, the reaction mixture was stirred in 1.5 liter of concentrated  $\text{NH}_4\text{OH}$  and nitrogen was led through for a period of 12 hours. The blue solution was filtered and the solid residue was washed with a little diluted  $\text{NH}_4\text{OH}$  solution and then with large amount of  $\text{H}_2\text{O}$  until the pH of filtrate close to 7. The crude olive-green product was dried in vacuum oven at ~ 60°C for one day. Crude yields ranged between 33 and 66 grams.

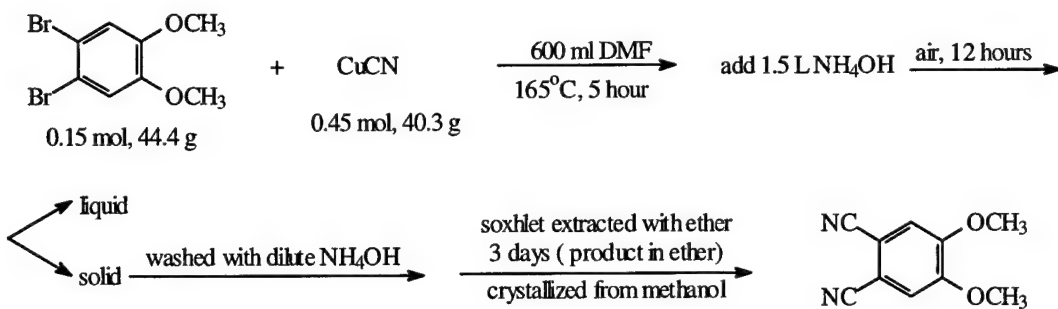


Figure 13. Synthesis and purification of 1,2-dicyano-4,5-dimethoxybenzene

The crude 1,2-dicyano-4,5-dimethoxybenzene has been purified by the procedure as shown in Figure 14. Pure 1,2-dicyano-4,5-dimethoxybenzene (30 grams, colorless needle-like crystals) were obtained using this approach.

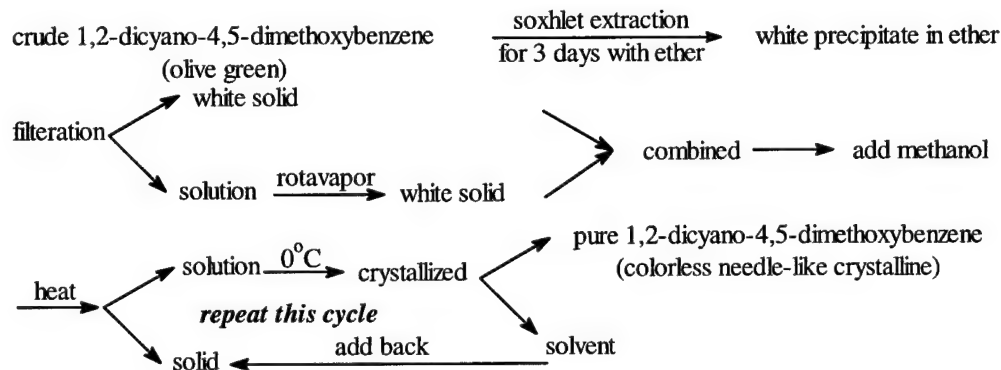


Figure 14. Purification of 1,2-dicyano-4,5-dimethoxybenzene

The purified 1,2-dicyano-4,5-dimethoxybenzene has been characterized by melting point and <sup>1</sup>H-NMR spectroscopy. Melting point: 166-168°C. <sup>1</sup>H-NMR (Figure 2, in CDCl<sub>3</sub>): 7.18 ppm (s, 2H, ArH); 4.00 ppm (s, 6H, OCH<sub>3</sub>). Literature data: m.p.: 179-181°C. 7.25 ppm(s, 2H, ArH); 3.97 ppm(s, 6H, OCH<sub>3</sub>).

### 2.1.3. Preparation of 2,3,9,10,16,17,23,24-(octamethoxyphthalocyaninato)Cu(II)

13.77 grams 1,2-Dicyano-4,5-dimethoxybenzene(0.073 mole) and 1.62 grams copper(II) chloride(0.012 mole) were heated in 180 mL of ethylene glycol at 200°C (reflux) for 5 hours, after which the reaction mixture was cooled somewhat, and an equal amount of H<sub>2</sub>O was added. The mixture was filtered while still hot, and the filtrate was

washed with hot water. The product was treated with 500 mL of 1N HCl and then with 500 mL of 1N NaOH, filtered and washed with water each time until the filtrate was of neutral pH. The solid material was then stirred in methanol, filtered and dried in vacuum oven at 60°C overnight. The yield was 2.33 grams of an olive green solid.

#### 2.1.4. Preparation of (2,3,9,10,16,17,23,24-Octahydroxyphthalocyaninato)Cu(II)

This compound has been prepared from (2,3,9,10,16,17,23,24-octamethoxy phthalocyaninato)Cu(II) by using two procedures. 300 mg of (2,3,9,10,16,17,23,24-octamethoxyphthalocyaninato) Cu(II) was heated under reflux in 8.0 grams of pyridine hydrochloride for half an hour. The reaction mixture was diluted with 80 mL of 10% aqueous HCl and stirred for 1 hour. After the solution was filtered and the residue was washed with water and acetone, the product was dried in vacuum overnight. Yield: 42 mg. A larger scale reaction was carried out starting with 1.8 grams of 2,3,9,10,16,17,23,24-octamethoxyphthalocyaninato Cu(II). Yield: 217 mg.

Since this procedure only resulted in low yield, an alternative procedure has been tried for this de-methylation reaction. 640 mg of 2,3,9,10,16,17,23,24-octamethoxy Pc Cu(II) was heated under reflux in 60 mL of toluene together with 2.09 g of AlCl<sub>3</sub> for half an hour. After the solution was cooled to room temperature, 100 mL of 10% HCl was added and the mixture was stirred for 1 hour. The solid was filtered off, washed with water, acetone and dried in vacuum oven overnight. Black powder, yield: 162 mg.

#### 2.1.5. Synthesis and purification of [2,3,9,10,16,17,23,24-octakis(11-hydroxyundecoxy) phthalocyaninato] copper(II) (CuPc[O(CH<sub>2</sub>)<sub>12</sub>OH]<sub>8</sub>)

150 mg of 2,3,9,10,16,17,23,24-octahydroxy phthalocyaninato Cu(II) was solubilized with 0.44 gram of 11-bromo-1-undecanol in 7.0 mL of DMSO and evacuated. To this

mixture was added 0.24 g of  $K_2CO_3$ . The mixture was evacuated again and heated at 100°C for 1 week. The reaction mixture was boiled with 40 mL of water, filtered, and washed with water and ether. After it was dried under vacuum overnight (crude product 290 mg), the residue was treated in a Soxhlet apparatus with acetone and chloroform for 48 hours. 110 mg of the product (as a black powder) was obtained.

Subsequent scaling up of the above procedures at each step eventually gave 1.4 grams of the octahydroxy product. It was found it could be purified by recrystallization from chloroform, significantly shortening the purification timescale. The purified complex was characterized by differential scanning calorimetry (DSC). The first and second heating DSC thermograms of this complex are shown in Figures 15 and 16. The first heating ramp shows broader transitions than the second, so the material reconsolidates into a more ordered structure upon the initial melt. The reappearance of the phase transitions in the second scan demonstrates the reversibility of the transitions between crystalline, liquid crystalline and isotropic phases in the alcohol substituted material.

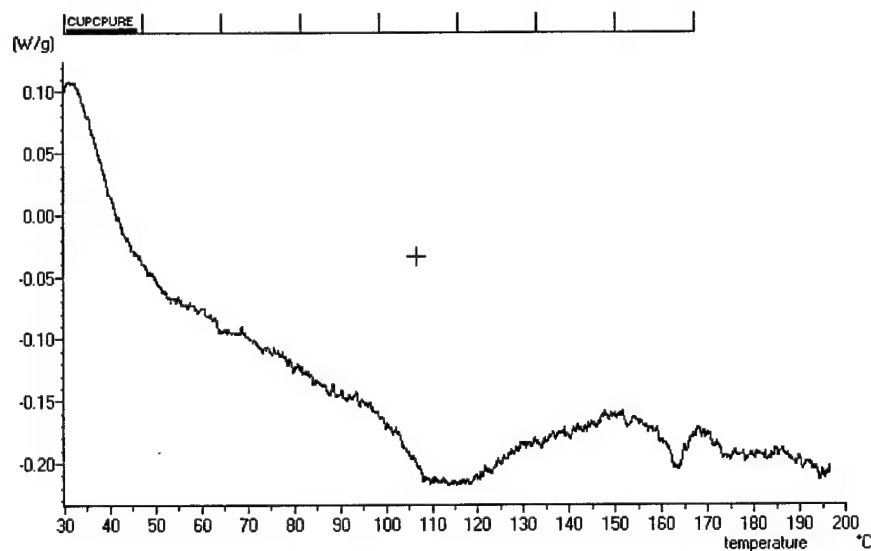


Figure 15. First heating DSC of  $CuPc[O(CH_2)_{12}OH]_8$ :

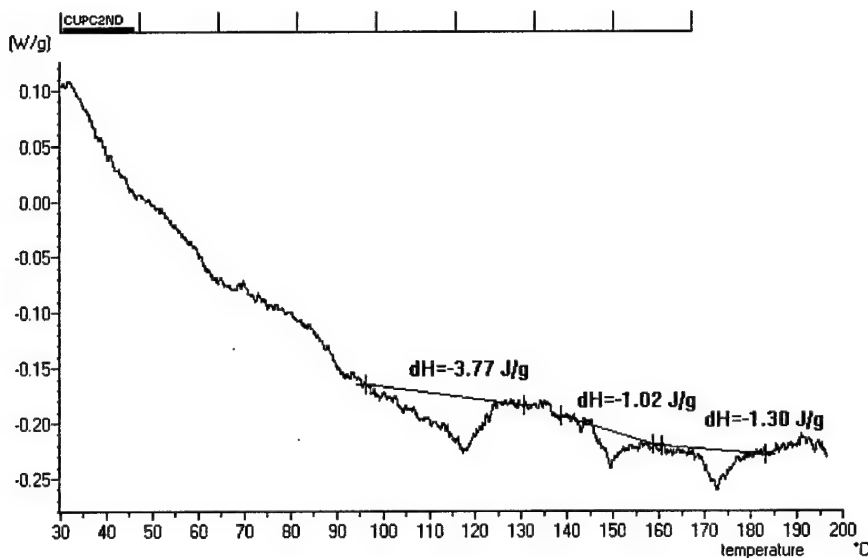


Figure 16. Second heating scan of  $\text{CuPc}[\text{O}(\text{CH}_2)_{12}\text{OH}]_8$ .

#### 2.1.6. Attempted epoxidation of [2,3,9,10,16,17,23,24-octakis(11-hydroxyundecoxy)phthalocyaninato] copper(II) ( $\text{CuPc}[\text{O}(\text{CH}_2)_{12}\text{OR}]_8$ ) with epichlorohydrin

The epoxidation of  $\text{CuPc}[\text{O}(\text{CH}_2)_{12}\text{OR}]_8$  was attempted in two steps via reaction with epichlorohydrin in the presence of catalytic  $\text{BF}_3\cdot\text{OEt}_2$  followed by dehydrohalogenation of the intermediate product formed by using  $\text{NaAlO}_2$ . The general approach for a number of small scale reactions involved dissolving the hydroxylundecanoxy substituted CuPc monomer into ethylene glycol dimethyl ether (DME) in the presence of an excess of epichlorohydrin. About 5%  $\text{BF}_3\cdot\text{OEt}_2$  was added and the mixture would be heated to 70 °C for 2-6 hours. The solvent would be removed *in vacuo* and replaced with an equivalent amount of THF. A stoichiometric amount of  $\text{NaAlO}_2$  would subsequently be added and the mixture heated for an additional 5-24 hours. The THF was removed by vacuum distillation. The crude materials were not soluble in chloroform (previously used to recrystallize the octahydroxy derivative) or other common solvents. An IR spectrum of the crude materials did not indicate the presence of significant amounts of oxirane

functionality (*ca.* 914-918 cm<sup>-1</sup>). It is believed the material either polymerized or decomposed.

### 2.1.7 Summary of the progress in the epoxy derivatized Pc monomer synthesis

The poor yields through the synthetic sequence and the inability to easily functionalize the CuPc monomer with epichlorohydrin using a conventional approach was frustrating. It might still be possible to obtain a cross-linkable matrix by incorporating acrylate termination on the long, flexible alcohol terminated arms of the Pc monomer, or to use a two step alkylation with an  $\alpha,\omega$ -bromoalkene followed by peroxidation to generate the desired epoxy monomer. However, the synthetic difficulty in obtaining reasonable amounts of material make this a commercial non-starter, and the efforts were subsequently directed into investigating alternative structures for polymerizable discotic LC monomers

## 2.2 Synthesis of Discotic Liquid Crystalline Metallodiketonate Monomers

The  $\beta$ -diketonate ( $\beta$ d) system is a planar metal complexing ligand, similar in geometry to the Pc materials (see Figure 8). The complexes consist of two substituted, acidic  $\beta$ ds that are deprotonated in order to bind to the metal ion. The conjugated nature of the ketonate chelate group and the stable square planar configuration of the metal ion result in an extremely stable complex. Our studies of the unbridged diketonates focused on the Cu substituted material since it has been shown to have excellent thermal stability and good mesophasic properties.

Substitution with alkyl chains of 10-12 carbon atoms in length at the eight positions shown has resulted in hexagonal discotic materials with solid to LC transitions at 70-110 °C and discotic to isotropic clearing temperatures of 130-140 °C.<sup>18</sup> It was hoped that

substitution with epoxy containing side chains should yield materials with similar properties.

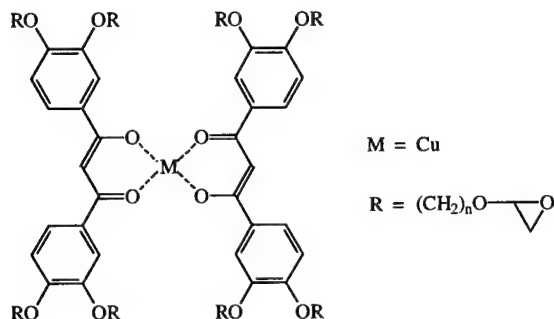


Figure 17.  $\beta$ -Diketonate Metal Complex with Epoxy Functionalization

The generalized synthetic approach to the  $\beta$ -diketonate copper complex is shown in Figure 17. The two starting materials are prepared by literature procedure, modified to include epoxy groups at the end of the alkyl chains.<sup>19</sup> Coupling of the acetyl and the methyl ester in the presence of a strong base yields the diketone in the enol form, which

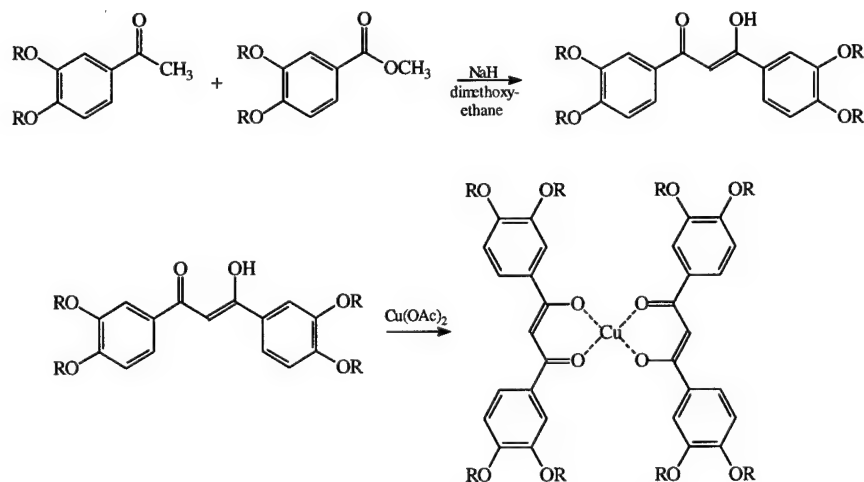


Figure 18. General synthetic approach to a discotic  $\beta$ -diketonate complex with epoxy modified pendant alkyl chains.

can then be complexed to the metal ion by addition of copper acetate. The diketonates can be prepared in high yield and low cost and, consequently, represented an attractive alternative discotic mesogen to the  $P_c$  system described above.

The synthetic work in the  $\text{Pc}$  system demonstrated to us that we needed to consider at least two specific approaches to obtaining the epoxy derivatized diketonate monomer. The first involved the coupling reaction of the methoxy protected precursors, followed by demethylation and derivatization with long chain aliphatic  $\alpha,\omega$ -bromoalcohols. Subsequent derivatization of the pendant aliphatic hydroxyls with epichlorohydrin catalyzed by  $\text{BF}_3$ -etherate, followed by dehydrohalogenation with sodium hydroxide would likely yield the deprotonated  $\beta$ -diketonate monomer with oxirane terminated arms. The first approach is shown in Figure 19 below. The second approach was designed to circumvent the difficulties observed using the epichlorohydrin route in the  $\text{Pc}$  system. This route involves attaching an  $\alpha,\omega$ -bromoalkene to each of the aromatic hydroxyl groups followed by oxidation with meta-chloro peroxybenzoic acid to yield the requisite oxirane functionality. Figure 20 illustrates this route, which was found to be preferable to the epichlorohydrin route. Additionally, Figure 20 shows a slight modification made to the benzoate methyl ester precursor in which a symmetric pyrogallol (3,4,5) substitution pattern was used compared to the catechol (3,4) structure shown in Figure 19. This protected precursor was readily available commercially, and allowed for incorporation of asymmetry to one side of the mesogen structure for the purposes of lowering the melting point of the resulting resin.

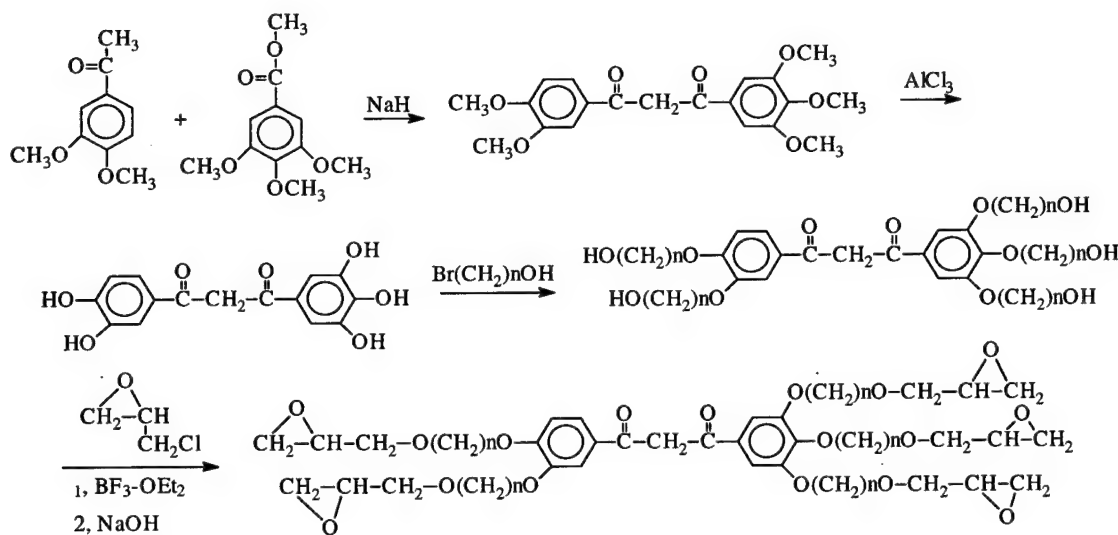


Figure 19. Epichlorohydrin route for the synthesis of di-ketone ligand with pendant epoxy groups.

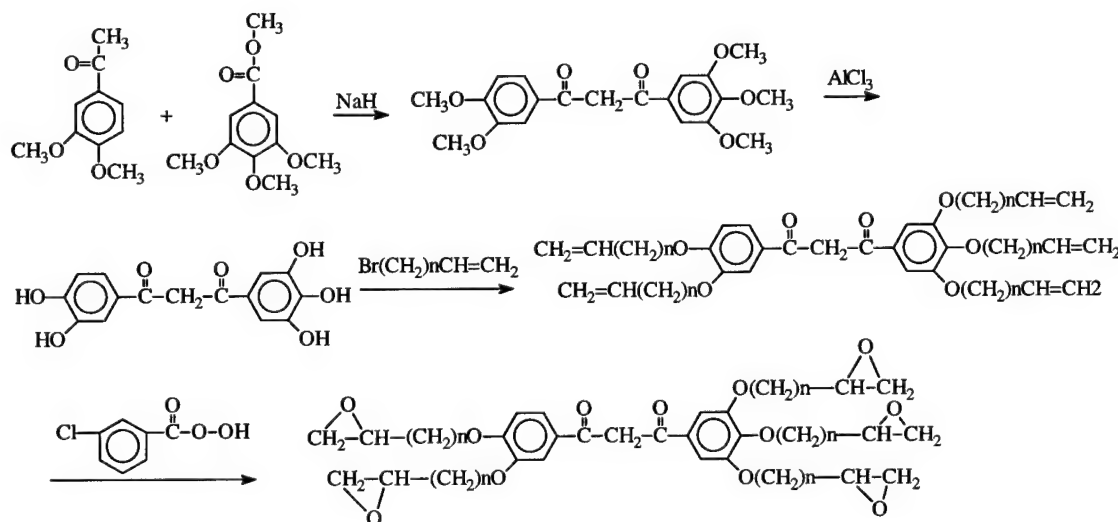


Figure 20. Peroxidation method for the synthesis of the di-ketone ligand with pendant epoxy groups.

## 2.2.1 Preparation of 1-(3',4'-dimethoxyphenyl)-3-(3",4",5"-trimethoxyphenyl)-propane-1,3-dione

The diketone product shown in Figure 21 has been prepared by the following one step procedure. A mixture of 6.73 grams of 3',4'-dimethoxyacetophenone and 8.45 grams of methyl 3,4,5-trimethoxybenzoate was dissolved in dry dimethoxyethane and was refluxed

for 3 hours in the presence of 5.4 grams sodium hydride. The resulting brown yellow-solution was cooled and poured into ice/H<sub>2</sub>O/HCl, where the excess NaH was quenched and the diketone was neutralized. The product was extracted with two 100 mL portions of diethyl ether and washed with distilled water. After the ether solution was dried with MgSO<sub>4</sub>, it was evaporated to give deep yellow liquid, which turned into a solid after standing overnight. Yield: 91%. The melting point range of this compound is 90-92°C.

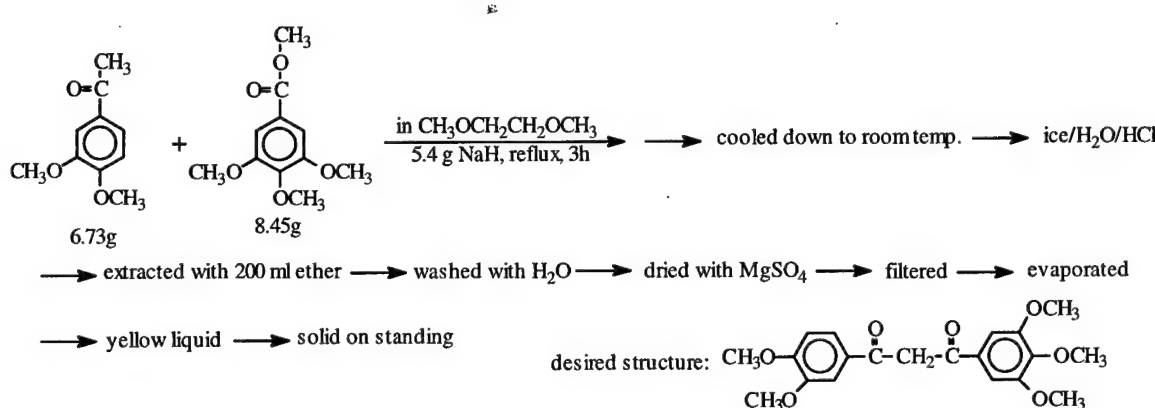


Figure 21. 1-(3',4'-dimethoxyphenyl)-3-(3'',4'',5''-trimethoxyphenyl)propane-1,3-dione preparation

Starting with 18.02 grams of 3',4'-dimethoxy-acetophenone and 22.62 grams of methyl 3,4,5trimethoxybenzoate, 35.55 grams of 1-(3'4'-dimethoxyphenyl)-3-(3'',4'',5''-trimethoxyphenyl)propane-1,3-dione were obtained.

#### 2.2.2. Cu(II) complex of 1-(3'4'-dimethoxyphenyl)-3-(3'',4'',5''-trimethoxyphenyl)-propane-1,3-dione

The Cu(II) complex of 1-(3'4'-dimethoxyphenyl)-3-(3'',4'',5''-trimethoxyphenyl)-propane-1,3-dione has been prepared by the following procedure (Figure 22). A mixture of 3.74 grams of 1-(3'4'-dimethoxyphenyl)-3-(3'',4'',5''-trimethoxyphenyl)propane-1,3-dione ligand, 1 gram of hydrated copper acetate, and 100 mL of ethanol/H<sub>2</sub>O (50%) was stirred for 2 hours and then boiled for 10 minutes. A yellow-green solid precipitated

when the reaction mixture was cooled to room temperature. The product was filtered and washed with methanol to give 1.87 gram of a yellow-green solid. The melting point of this complex is 227-230°C.

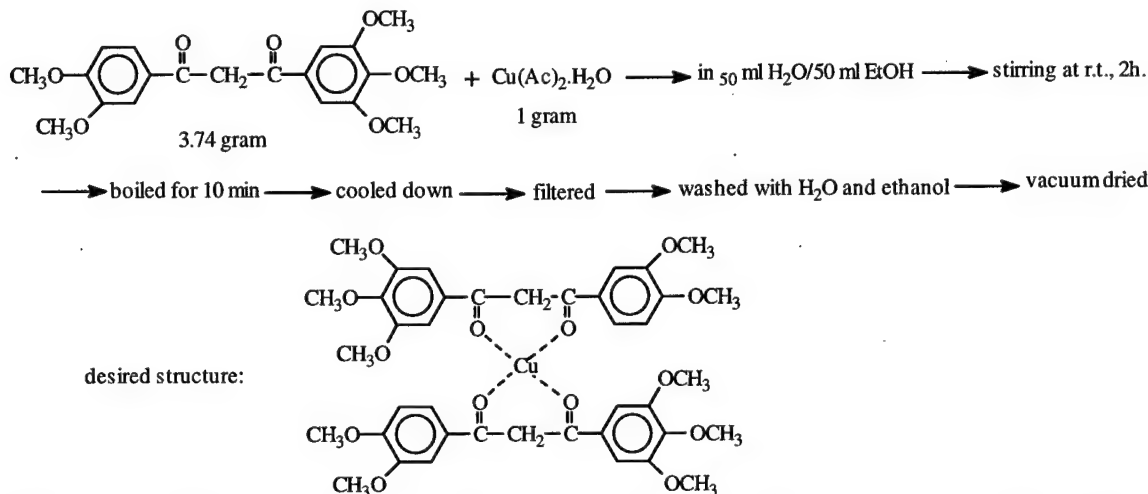


Figure 22. Bis[1-(3',4'-dimethoxyphenyl)-3-(3'',4'',5''-trimethoxyphenyl)propane-1,3-dioato] copper(II) complex preparation

### 2.2.3. Demethylation of 1-(3',4'-dimethoxyphenyl)-3-(3'',4'',5''-trimethoxyphenyl)propane-1,3-dione using AlCl<sub>3</sub>

A round bottom flask was charged with 4.00 grams of 1-(3',4'-dimethoxyphenyl)-3-(3'',4'',5''-trimethoxyphenyl) propane-1,3-dione and 100 mL of toluene. After the material was dissolved with stirring, 8.00 grams of AlCl<sub>3</sub> were added and the reaction mixture brought to reflux for one hour. After cooling to room temperature, a white precipitate formed. The product (1.57 grams) was isolated by suction filtration and washed with water. Melting point range: 100-104°C. A larger scale reaction utilized 15.0 grams of 1-(3',4'-dimethoxyphenyl)-3-(3'',4'',5''-trimethoxyphenyl) propane-1,3-dione and 30.0 grams of AlCl<sub>3</sub>. Isolated yield of the white solid was 10.18 grams. Melting point range: 100-104 °C.

2.2.4. Reaction of 1-(3'4'-dihydroxyphenyl)-3-(3",4",5"-trihydroxyphenyl) propane-1,3-dione with Br(CH<sub>2</sub>)<sub>12</sub>OH

A round bottom flask was charged with 0.50 grams of 1-(3'4'-dihydroxyphenyl)-3-(3",4",5"-trihydroxyphenyl) propane-1,3-dione, 25 mL of dimethylformamide (DMF), 0.40 grams of potassium carbonate (K<sub>2</sub>CO<sub>3</sub>) and 2.06 grams of Br(CH<sub>2</sub>)<sub>12</sub>OH. The reaction mixture was heated to 90 °C with stirring for 3 hours and then poured onto ice. Upon melting the ice, the reaction mixture was heated to boiling briefly (5 minutes). The crude product (1.66 grams) was isolated by suction filtration. A white solid (0.90 grams) was obtained after recrystallization from acetone. A scaled up reaction using the conditions described above utilized 4 grams of 1-(3'4'-dihydroxyphenyl)-3-(3",4",5"-trihydroxyphenyl) propane-1,3-dione, 3.2 grams of K<sub>2</sub>CO<sub>3</sub>, 200 mL of DMF and 16.5 grams of Br(CH<sub>2</sub>)<sub>12</sub>OH. The crude yield was 14.74 grams. After recrystallization, the yield of pure material was 10.49 grams. Melting point range: 68-72 °C. The <sup>1</sup>H NMR spectrum was consistent with the desired structure.

2.2.5. Preparation of bis[1-(3',4'-dihydroxy-undecanoxyphenyl)-3-(3",4",5"-trihydroxyundecanoxyphenyl) propane-1,3-dionato]copper(II)

The intended structure of the title complex is depicted in Figure 23 below. Cu(II) complexes with two identical β-diketonate ligands predominantly adopt square planar coordination geometries about the Cu atom. The appreciable steric hinderance likely to be present within a coordination plane, with two of the rings having both the 3- and 5-positions substituted with a long flexible linker arm, may disrupt the square planar geometry favored by a d<sup>9</sup> electronic configuration at the metal center. At the time of the synthetic work, no molecular modeling of the expected structure had been carried out.

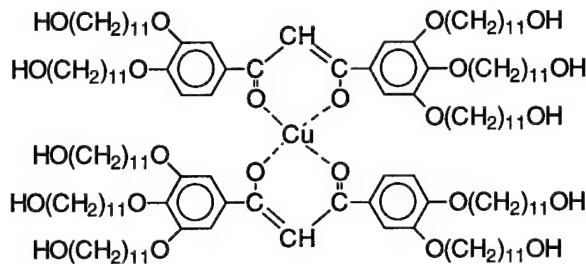


Figure 23. The structure of 1-(3',4'-dihydroxyundecanoxyphenyl)-3-(3'',4'',5''-trihydroxyundecanoxyphenyl) propane-1,3-dione

A mixture of 1.224 gram 1-(3',4'-dihydroxyundecanoxyphenyl)-3-(3'',4'',5''-trihydroxyundecanoxyphenyl)propane-1,3-dione, 0.1 gram hydrated copper acetate and 40 ml of ethanol was stirred and refluxed for 3 hours. The reaction mixture was cooled to room temperature and evaporated to dryness. 30 mL of methanol was added and the solution was stored in a 4°C refrigerator overnight. The precipitated green solid was filtered and dried in a vacuum oven to a constant weight. The isolated yield of the green solid was 0.53 grams. The reaction was scaled up with 6.85 grams of 1-(3',4'-dihydroxyundecanoxyphenyl)-3-(3'',4'',5''-trihydroxyundecanoxyphenyl)propane-1,3-dione and 0.94 gram hydrated copper acetate. The isolated yield was 4.06 grams after recrystallization from acetone.

#### 2.2.6. DSC analysis of Bis[1-(3',4'-dihydroxyundecanoxyphenyl)-3-(3'',4'',5''-trihydroxyundecanoxyphenyl) propane-1,3-dionato]copper(II)

Two peaks were observed at 67 and 107 °C during the first heating scan in the DSC roughly corresponding to K→D and D→I transitions respectively (“K” is crystalline, “D” is discotic, and “I” is isotropic) as shown in Figure 24. The second heating scan in the DSC Figure 25 also showed the expected liquid crystal properties, although the transitions sharpened and the peaks shifted to lower temperature. In addition, birefringence of this compound at both 60 and 85°C was observed by microscopy

indicating a preservation of crystalline ordering. The shifting and sharpening of the peaks implies that the initial melting of the compound in the DSC and subsequent slow cooling to room temperature allowed the material to relax back into a more ordered state than it had initially. The second DSC thermogram (Figure 25) shows that another

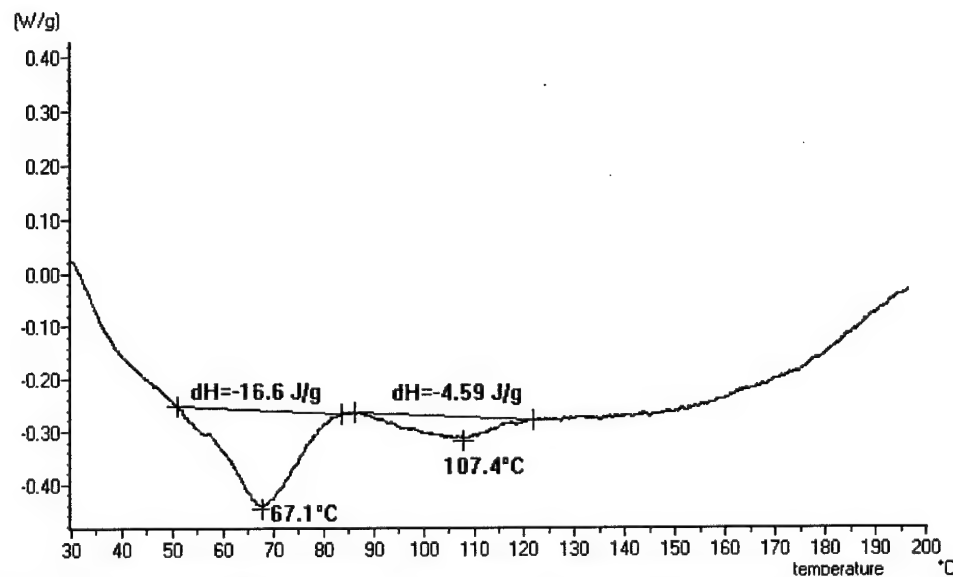


Figure 24. First heating DSC thermogram of bis[1-(3',4'-dihydroxyundecanoxyphenyl)-3-(3'',4'',5''-trihydroxyundecanoxyphenyl)propane-1,3-dionato]copper(II). Heating rate was 10°C/min.

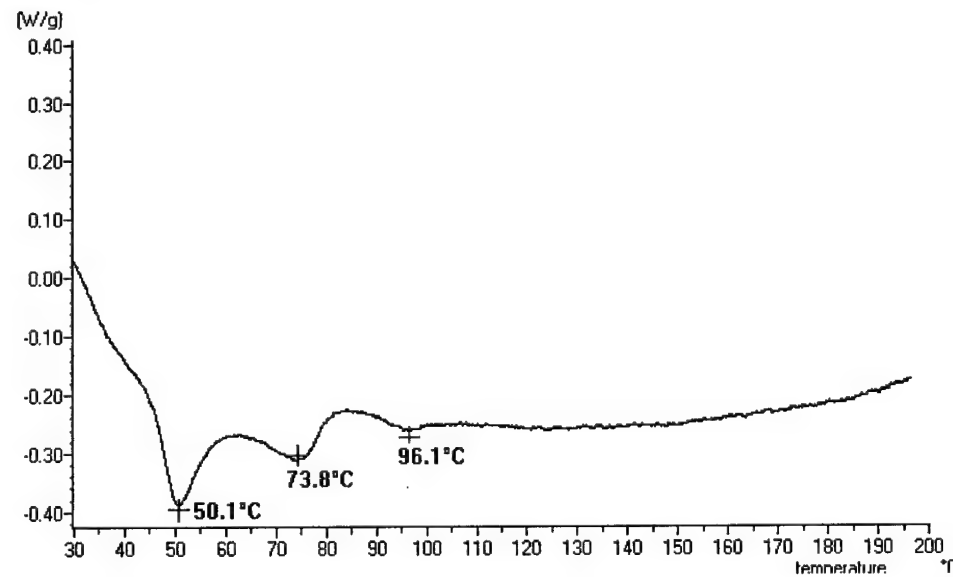


Figure 25. Second heating DSC of bis[1-(3',4'-dihydroxyundecanoxyphenyl)-3-(3'',4'',5''-trihydroxyundecanoxyphenyl)propane-1,3-dionato]copper(II). Heating rate 10 °C/min.

transition is clearly visible, probably corresponding to  $K \rightarrow N_c$  (50 °C),  $N_c \rightarrow N_d$  (74 °C), and  $N_d \rightarrow I$  (96 °C) transitions respectively, where  $N_c$  is nematic columnar and  $N_d$  is nematic discotic (see Figures 3 and 4).

#### 2.2.7. Attempted epoxidation of 1-(3',4'-dihydroxyundecanoxyphenyl)-3-(3",4",5"-trihydroxyundecanoxyphenyl) propane-1,3-dione using epichlorohydrin.

The initial attempts at epoxidation of 1-(3',4'-dihydroxyundecanoxyphenyl)-3-(3",4",5"-trihydroxyundecanoxyphenyl) propane-1,3-dione with epichlorohydrin used the two step process illustrated in Figure 26. An example reaction to illustrate the procedure is given here. In the first step, 2.45 grams of 1-(3',4'-dihydroxy-undecanoxyphenyl)-3-(3",4",5"-trihydroxyundecanoxyphenyl) propane-1,3-dione and 1.11 grams of epichlorohydrin were placed in a 50 mL round bottomed flask and 25 mL of DME was added. The reaction mixture was heated to 50~60°C and 0.1 grams of  $BF_3 \cdot OEt_2$  was added as to catalyze the ring opening addition reaction. After about 2 hours, the reaction

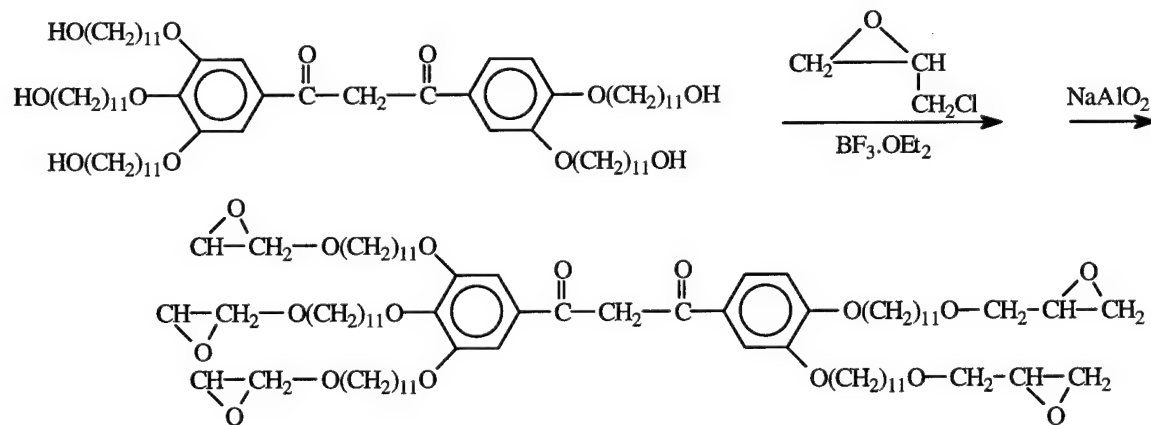


Figure 26. Epoxidation of 1-(3',4'-dihydroxyundecanoxyphenyl)-3-(3",4",5"-trihydroxyundecanoxyphenyl) propane-1,3-dione with epichlorohydrin and  $NaAlO_2$ . vessel was cooled to room temperature and the solvent was evaporated using a liquid nitrogen cooled vacuum trap.

In the dehydrohalogenation step, 20 mL of tetrahydrofuran was added to the crude product isolated from first step. A clear solution was formed after the stirred reaction mixture was heated to 50 °C. At that point, 0.54 grams of NaAlO<sub>2</sub> was added into the solution. The reaction mixture was maintained at 60°C for 6 hours with magnetic stirring. The reaction mixture was cooled to room temperature, and the solid which precipitated was filtered off and the solvent was evaporated to give a yellow solid residue.

After checking the <sup>1</sup>H NMR spectrum and the IR spectrum of the product, it seems that no epoxy groups had been incorporated into the compound. Thus, modification of the reaction conditions were required for this reaction.

#### 2.2.8 Partial epoxidation of 1-(3',4'-dihydroxyundecanoxyphenyl)-3-(3",4",5"-trihydroxyundecanoxyphenyl) propane-1,3-dione using epichlorohydrin.

Modifications to the procedure listed in section 2.2.6 (above) included using a higher reaction temperature (70 °C instead of 50 °C), a longer reaction time (6 hrs vs. 2 hrs) and isolation of the initial epichlorohydrin addition product prior to the dehydrohalogenation step. We also used longer reaction times for dehydrohalogenation (24 hrs vs. 6 hrs). All purification procedures were carried out at room temperature. The product thus obtained is a viscous liquid, physically different from that obtained in the previous procedure. The crude product was purified by reprecipitation from chloroform with hexane.

In an attempt to determine the epoxy group content per molecule, the reaction product was reacted with pyridine-HCl in pyridine for a few hours. After the reaction, the excess HCl was titrated by a standardized KOH solution using phenolphthalein as indicator. Thus, 0.11 grams of the recrystallized epoxy product was reacted with 10 mL of 0.1 N

pyridine-HCl in pyridine for 1.5 hr at 80 °C. The reaction mixture was cooled down to room temperature and titrated with 0.0967 N KOH-methanol standard solution. 9.50 ml of the KOH solution was used and the calculated epoxy content was 1352 g/mol. Since the product has deep yellow color, we did not obtain very accurate results from titration. However, <sup>1</sup>H NMR analysis showed about 30% to 35% of oxirane content was present in the sample based on the total functionality.

We also carried out the epoxidation reaction under the following different reaction conditions varying temperature and the epichlorohydrin/hydroxyl (ECH/OH) ratio:

- i) 1<sup>st</sup> step: 50-60°C, 2hr., ECH/OH ~1.5, 2<sup>nd</sup> step: 50°C, 6-7 hr.;
- ii) 1<sup>st</sup> step: 70°C, 6hr., ECH/OH ~1.5, 2<sup>nd</sup> step: 60°C, 24hr.;
- iii) 1<sup>st</sup> step: 80°C, 6hr., ECH/OH ~1.5, 2<sup>nd</sup> step: 60°C, 24hr.

The epoxy contents were 0, 33%, 35% respectively. Comparing ii) and iii), a further increase of the reaction temperature resulted in only a slight increase in the epoxy content. Increasing the epichlorohydrin content to 2.5 compared to free hydroxyl groups showed that the epoxy percentage was increased to a maximum of about 40% according to <sup>1</sup>H NMR analysis.

#### 2.2.8. Acylation of 1-(3',4'-dihydroxyundecanoxyphenyl)-3-(3",4",5"-trihydroxyundecanoxyphenyl) propane-1,3-dione using acryloyl chloride.

The intent of this reaction was to introduce a cross-linkable group (using a free-radical initiator) into the new mesogenic structure. One gram (1.00 g) of bis[1-(3',4'-dihydroxyundecanoxyphenyl)-3-(3",4",5"-trihydroxyundecanoxyphenyl) propane-1,3-dionato]copper(II) was treated with 1.60 mL of acryloyl chloride in 20 mL of dry chloroform at room temperature for 48 hours. 1.1 grams K<sub>2</sub>CO<sub>3</sub> was added to neutralized

the acid formed. Initially, the reaction was heterogeneous. After the reaction, about 100 mL of water was added. The organic phase which contained the product was washed with H<sub>2</sub>O several times and then dried with anhydrous MgSO<sub>4</sub>. The organic phase was then removed using a rotary evaporator. Based on a loss of color, it appeared that the Cu(II) was leached from the structure under the reaction conditions. Thus, the diketone ligand was directly reacted with acryloyl chloride using a similar procedure as shown below (Figure 27). The Cu(II) complex was then prepared by reacting the acrylate substituted  $\beta$ -diketone with Cu(OAc)<sub>2</sub>.

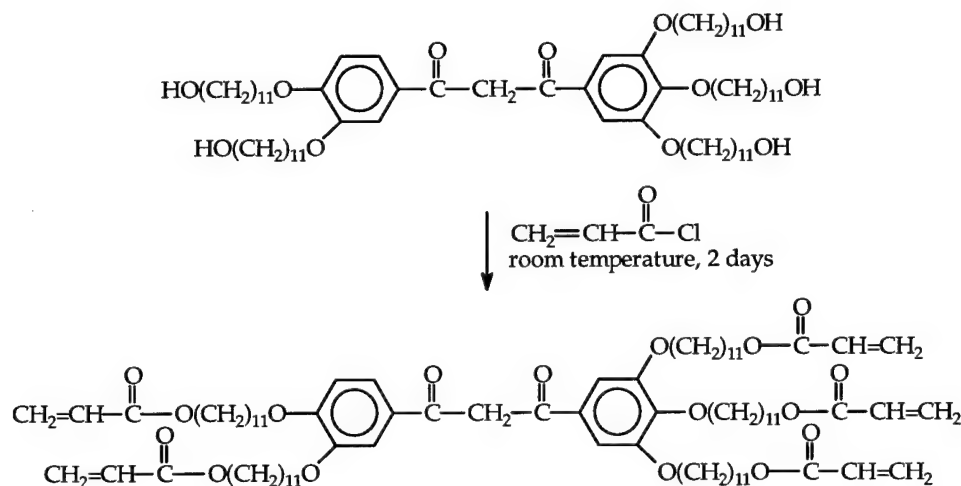


Figure 27. Acryloylation of the pentaalcohol  $\beta$ -diketone core.

After the reaction of the 1-(3',4'-dihydroxyundecanoxyphenyl)-3-(3",4",5"-trihydroxyundecanoxyphenyl)propane-1,3-dione with acryloyl chloride and potassium carbonate, the mixture was poured into H<sub>2</sub>O, and then washed with H<sub>2</sub>O several times, dried with anhydrous MgSO<sub>4</sub> for 2 hours, filtered, and evaporated to dryness. The reaction mixture was held at room temperature during the entire reaction to avoid polymerization of the acryloyl groups. A yellow, viscous liquid was obtained and <sup>1</sup>H NMR and showed that over 90% of the possible acryloyl groups were incorporated into

the structure. The acrylated diketone product was stirred with 0.5 equivalents of hydrated Cu(OAc)<sub>2</sub> in 50% ethanol/water at room temperature for 20 hours and then heated to boiling temperature for 5 minutes. After cooling down to room temperature, a viscous oil-like precipitate formed which was subsequently washed with a mixture of H<sub>2</sub>O/ethanol repeatedly and finally washed with 95% ethanol and dried in the air. The resulting complex is a very viscous liquid (semi-solid) with a yellow-green color. It has a different appearance from the Cu(II) complex of the diketone with terminal OH groups.

DSC analysis of this complex didn't show any peaks, indicating the absence of any liquid crystallinity above room temperature. The acrylate groups might affect the stability of both the mesophase and the crystalline phase via steric effects and unfavorable changes in the molecular dipole moment. The first effect should destabilize the crystalline phase, as it perturb the regular packing of the paraffinic peripheral chains. Such a phenomenon had been suggested in the literature to be responsible for the decrease in the crystal - to - mesophase transition temperatures observed for some Cu(II) carboxylates containing unsaturations in the middle or in the end of the peripheral chains, as compared to the linear aliphatic homologues. In contrast, the presence of dipolar intermolecular interactions may preclude the disordering of the aliphatic chains, which is necessary to efficiently fill the space in a liquid crystalline state. This second effect could be responsible for a destabilization of the liquid crystalline phase.

#### 2.2.9. Preparation of an epoxidized $\beta$ -diketone ligand via the procedure shown in

Figure 28 using a short flexible spacer group (n=6).

1-(3',4'-dihydroxyphenyl)-3-(3",4",5"-trihydroxyphenyl) propane-1,3-dione was reacted with 5.5 equivalents (10% excess) of 8-bromo-1-octene (n=6) in refluxing

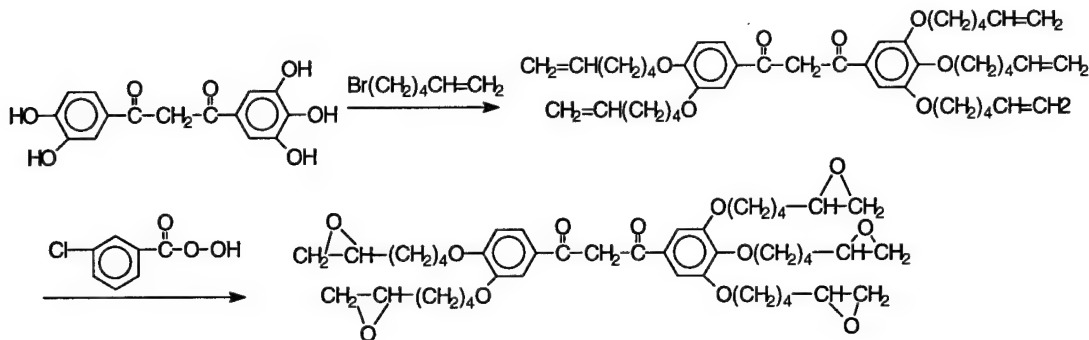


Figure 28. Reaction sequence for alkylating the pentaphenol mesogen core with an  $\alpha,\omega$ -bromoalkene and subsequent conversion to the pentaepoxide.

acetone using potassium carbonate as a deprotonating agent and 0.1 equivalents of 18-crown-6 as a phase transfer catalyst. The product was worked up after 24 hours to yield a dark oil which was taken up in hexane and purified by means of silica plug filtration to render the pentaolefin(PO)(n=6) as a red viscous oil in 30% yield. Epoxidation with m-chloroperoxybenzoic acid in chloroform, followed by dilution with an equal volume of petroleum ether and extraction with aqueous sodium hydrogen sulfite, then sodium hydrogen carbonate solution and finally water, produced a yellowish organic phase which, upon drying over sodium sulfate. The solvent was removed *in vacuo*, giving the pentaepoxide (PE)(n=6) in 80% yield as a red viscous oil.  $^1\text{H}$  NMR analysis provided evidence of essentially complete conversion of the pendant olefinic functional groups into oxirane moieties.

#### 2.2.10 Preparation of bis[PE(n=6)] complex of Cu(II)

The intended structure of the title complex is depicted in Figure 29 below. The procedure for the synthesis and purification of this complex was essentially identical to that given in section 2.2.5 above for the penta(alcohol) complex.

Unfortunately, the Cu(II) complex of the PE (n=6) ligand only shows *crystalline* behavior without formation of any mesophases when viewed under the polarized

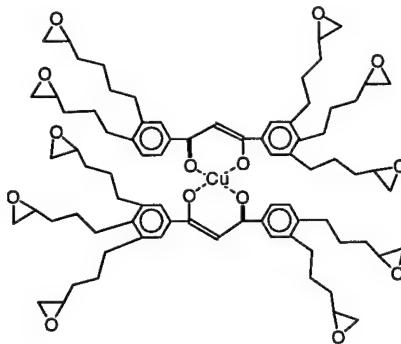


Figure 29. Square planar, bis-ligand Cu(II) complex of the fully epoxidized  $\beta$ -diketonate monomer. This material does not show any liquid crystalline phases.

microscope equipped with a hot stage. At 220 °C, the anisotropy of the crystal needles vanishes with non-recoverable destruction (due to thermal decomposition). This result does not come as a complete surprise, since the necessity of a critical side chain length of at least 8 carbon atoms has been previously reported with similar molecular structures. As expected, no endothermic phase transitions (melting or LC phase change) can be detected. Nevertheless, the feasibility of applying above described synthetic route for the preparation of longer chains than octenyl is obvious. Unfortunately, any  $\omega$ -bromo- $\alpha$ -olefin higher than 8-bromo-1-octene has to be synthesized because of the lack of commercial availability. Previous work as Aspen Systems has shown that this type of compound can be made in about 40% overall yield from  $\alpha$ ,  $\omega$ -dibromoalkanes through partial dehydrobromination with potassium t-butoxide in anhydrous tetrahydrofuran.

#### 2.2.11. Synthesis of $C_{10}$ -bromoolefin and its reaction with the $\beta$ -diketone core

As described above, the Cu(II) complex of PE( $n=6$ ) has been prepared and only shows crystalline behavior without indication of formation of a mesophase when viewed under the polarized microscope equipped with a hot stage. A longer spacer chain length ( $n>8$ ) was suggested to increase the percentage of flexible space. Thus, 12-Bromo-1-

dodecene( $n=10$ ) was prepared using the following procedure: A solution of 100 g 1,12-dibromo-dodecane (0.305 mol) in 150 ml tetrahydrofuran was treated at room temperature with a solution of 55.0 g potassium t-butoxide in 250 mL of tetrahydrofuran, followed by heating at reflux for 30 min. Upon cooling, the mixture was filtered to remove potassium bromide and subjected to solvent evaporation to yield an amber-colored oil. Vacuum distillation at  $\sim 3$  mmHg gives 22.5 g fraction 1 (1,11-dodecadiene, 41% yield), b.p. 79-80°C (3 mm Hg) and 23 g fraction 2 (12-bromo-1-dodecene, 30% yield), b.p. 127-128°C (3 mm Hg).  $^1$ H-NMR analysis of fraction 1(1,11-dodecadiene): 5.8ppm(2H, -CH=); 5.0ppm(4H, CH<sub>2</sub>=); 2.1ppm(4H, -CH<sub>2</sub>-CH=); 1.2-1.6ppm(12H, other CH<sub>2</sub>'s). Fraction 2 (12-bromo-1-dodecene): 5.8ppm(1H, -CH=); 5.0ppm(2H, CH<sub>2</sub>=); 3.4ppm(2H, Br-CH<sub>2</sub>-); 2.1ppm(2H, -CH<sub>2</sub>-CH=); 1.9ppm(2H, Br-CH<sub>2</sub>-CH<sub>2</sub>-), 1.2-1.6ppm(16H, other CH<sub>2</sub>'s) The 12-bromo-1-dodecene was reacted with 1-(3',4'-dihydroxyphenyl)-3-(3",4",5"-trihydroxyphenyl) propane-1, 3- dione under the reaction conditions described in section 2.2.9 above. Figure 30 shows the synthesis and product work-up procedures.

#### 2.2.12. Epoxidation of the $\beta$ -diketone with C<sub>12</sub> alkene substitutions and its copper(II) complex

The pentaalkene substituted diketone isolated using the procedure described in section 2.2.11 and shown in Figure 30 was epoxidized by the following procedure: 2.00 grams of penta-olefin substituted diketone was dissolved in 20 mL of chloroform. To this solution, 3.00 grams of 3-chloroperoxybenzoic acid (in 30 mL CHCl<sub>3</sub>) was added and the reaction mixture was stirred at room temperature for 2 hours. After the reaction, petroleum ether (150mL) was added and kept in refrigerator over night to precipitate 3-

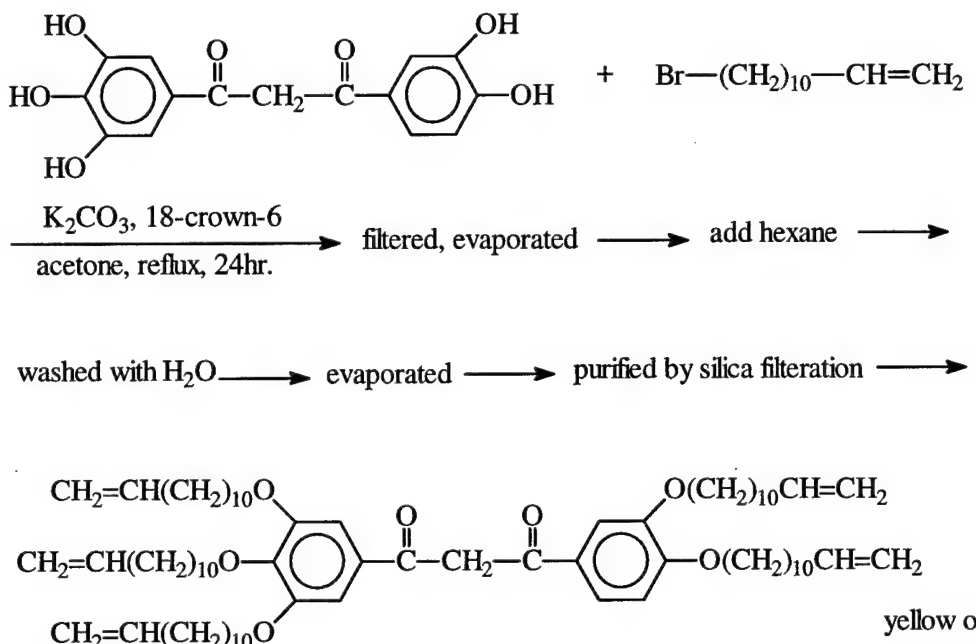


Figure 30. Synthesis and purification of long chain pentaalkene modified  $\beta$ -diketone.

chlorobenzoic acid and the excess 3-chloroperoxybenzoic acid. The solution was then filtered and washed with: 1) 10%  $\text{NaHSO}_3/\text{H}_2\text{O}$  solution twice; 2) 10%  $\text{NaHCO}_3/\text{H}_2\text{O}$  solution twice; and 3)  $\text{H}_2\text{O}$  several times. Then the solution was dried with anhydrous  $\text{MgSO}_4$  for a few hours. Finally, the solution was evaporated to dryness. A light yellow oily solid (1.92 grams) was obtained.

The above epoxy  $\beta$ -diketone has been used to prepare its copper(II) complex by the method previously described in section 2.2.5. DSC analysis and polarized light microscopy using a hot stage showed that no liquid crystalline was present above room temperature.

#### 2.2.13. Synthesis of the $\beta$ -diketone ligand with $-\text{O}-(\text{CH}_2)_9\text{OH}$ substitutions and its complex with Cu(II)

The diketone has been prepared by using the procedure illustrated in Figure 31 below, in a fashion similar to that previously described for the diketone with longer alkyl

substitutions. 3.04g 1-(3',4'-Dihydroxyphenyl)-3-(3",4",5"-trihydroxyphenyl) propane-1,3-dione and 11.16g 9-bromo-1-nonanol were used as starting materials. The obtained product is a very viscous liquid.

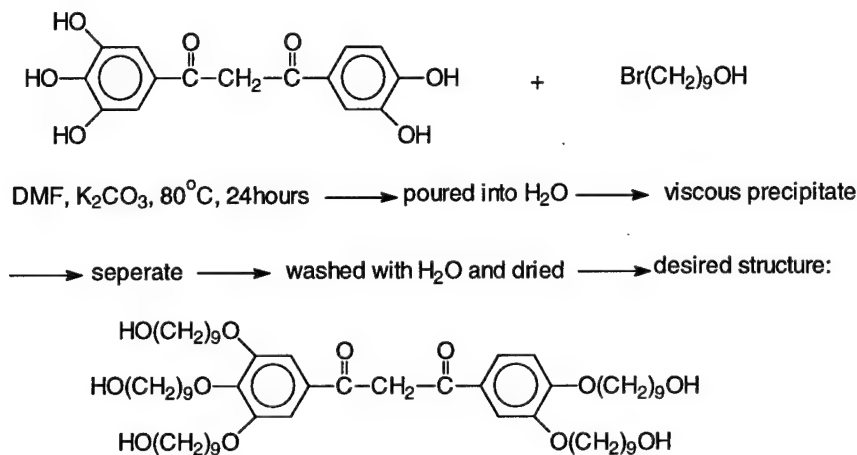


Figure 31. Synthesis and isolation pathway for the  $\beta$ -diketone core with  $-O-(CH_2)_9OH$  substitutions.

The copper(II)-diketone with  $C_9$  substitutions(OH type) complex was prepared by using the same procedure as described before. The complex obtained is a yellow-green semi-solid. DSC investigation of above prepared complex has been performed. Both the first and second heating thermograms did not show any evidence of liquid crystallinity.

#### 2.2.14. Summary of the work with the $\beta$ -diketone structure

Although promising synthetic routes have been developed for the hydroxyl substituted  $\beta$ -d mesogenic core structure, it is clear that the modifications to date with flexible spacer groups and either terminal epoxide or acrylate functionalities failed to give an LC resin. It is possible that following up on one of the areas described above that the appropriate spacer groups and functional groups could be discovered to generate a useful discotic LC resin. However, it was decided that a fundamental switch to a different mesogen core structure was likely to yield positive results in less time.

## 2.3 Cu(II) carboxylate metallomesogens

In order to expand the material candidates for thermally conductive composite application, a new family of thermoset monomers was designed (Figure 32). These new monomers include hydroxyl, epoxy and vinyl-terminated carboxylate copper(II) complexes.

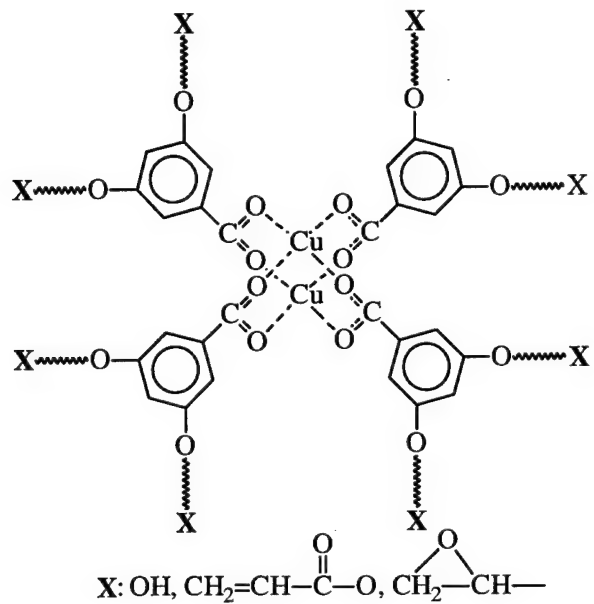


Figure 32. Next generation design for discotic LC thermoset monomers.

General synthetic approaches to achieve the core structures shown in Figure 32 are shown in Figures 33 and 34 below. It was anticipated that these monomers would form binuclear complexes based on numerous literature precedents for Cu(II) complexes of substituted carboxylates (non-polymerizable) as shown in Figure 35.

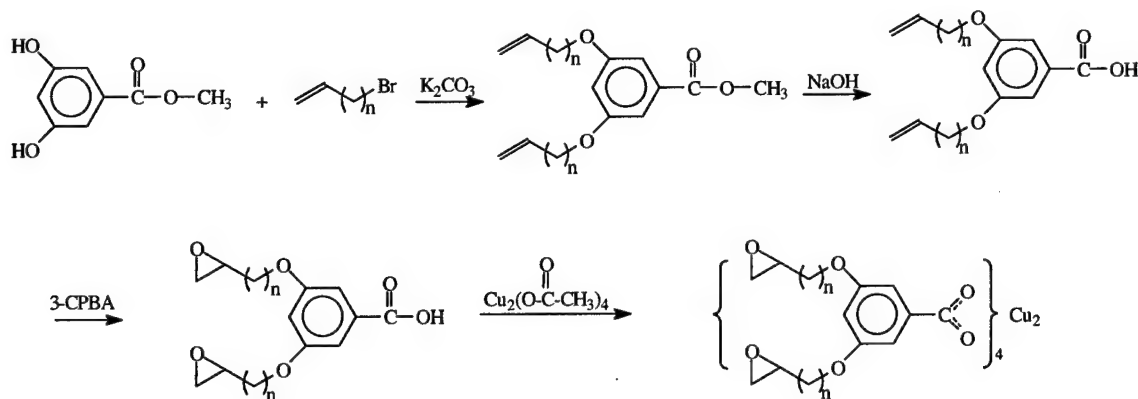


Figure 33. Synthetic pathway to the 8-arm epoxy substituted discotic LC thermoset based on Cu(II) coordinated substituted carboxylates.

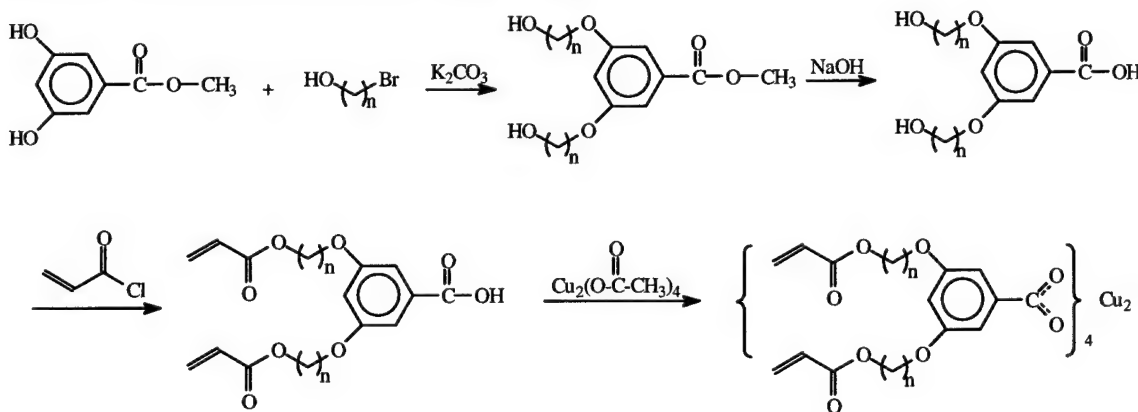


Figure 34. Synthetic pathway to the 8-arm acrylate substituted discotic LC thermoset based on Cu(II) coordinated substituted carboxylates.

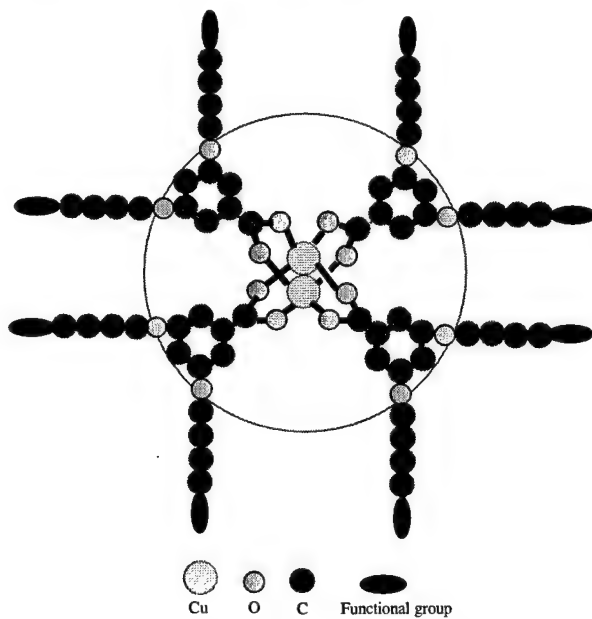


Figure 35. Idealized structure of the Cu<sub>2</sub>(OCOR)<sub>4</sub> discotic LC thermosets.

### 2.3.1. Acrylated substituted discotic LC thermosets

#### 2.3.1.1. Methyl 3,5-bis(11-hydroxyundecanoxy) benzoate.

This compound was synthesized by the following procedure (Figure 36): A mixture was prepared with 4.2 grams of methyl 3,5-hydroxybenzoate, 12.55 grams of 1-bromo-11-undecanol, and 6.9 grams of  $K_2CO_3$  in 50 mL of DMF. This suspension was heated at 80 °C for 24 hours. After cooling, the reaction mixture was poured into 150 mL of water, stirred for 3 hours at room temperature and filtered. The filtered solid (crude product) was purified by recrystallization from acetone. A light yellow solid was obtained. Yield: 9.3 grams.

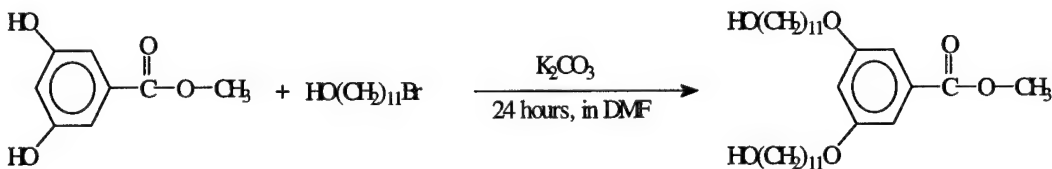


Figure 36. Synthesis of methyl 3,5-bis(11-hydroxyundecanoxy) benzoate

#### 2.3.1.2. 3,5-Bis(11-hydroxyundecanoxy)benzoic acid.

This compound was prepared by the procedure indicated in Figure 37. A round bottom flask was charged with 8.0 grams of methyl 3,5-bis(11-hydroxyundecanoxy) benzoate and 7.1 grams of NaOH in 200 mL ethanol and refluxed for 4 hours. The mixture was then cooled down to room temperature. The solution was then neutralized with an aqueous solution of hydrochloric acid, and the precipitated 3,5-bis(11-hydroxyundecanoxy) benzoic acid was isolated by suction filtration. Yield: 6.42 grams.

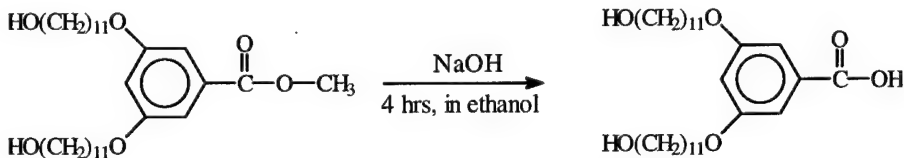


Figure 37. Synthesis of 3,5-bis(11-hydroxyundecanoxy) benzoic acid

#### 2.3.1.4 Hydroxyl substituted discotic LC mesogen: Copper 3,5-bis(11-hydroxy-undecanoxy) benzoate

The structure of the title complex is shown in Figure 38. To a solution of 3,5-bis(11-hydroxyundecanoxy) benzoic acid (1.5 grams in 30 ml H<sub>2</sub>O), 0.303 grams of Cu(OAc)<sub>2</sub>·H<sub>2</sub>O (in ~20 ml H<sub>2</sub>O) was added. The reaction mixture was then stirred at room temperature for 20 hours. A green solid precipitated over the course of the reaction and was subsequently filtered at room temperature. The product was washed with ethanol several times and dried in a vacuum oven overnight. Yield: 0.80 grams.

The DSC thermogram of the isolated dicopper complex depicted in Figure 38 is provided in Figure 39. The complex clearly showed liquid crystal behavior. The birefringent behavior of this complex was observed at both 140°C and 160°C, as shown in the microscopy images in Figures 40 and 41 respectively.

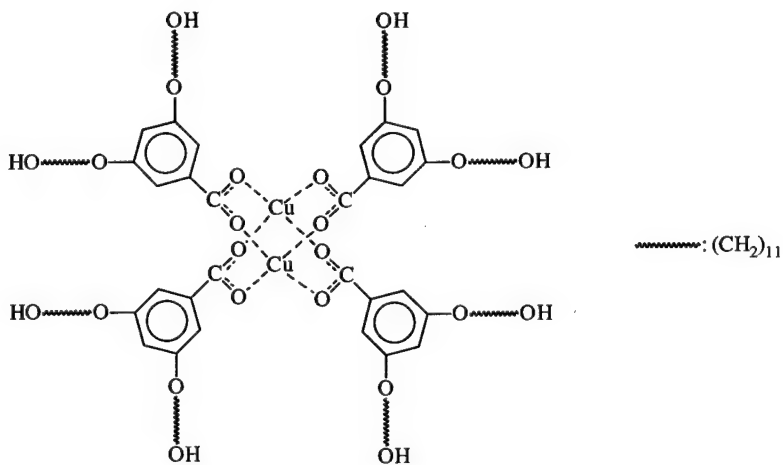


Figure 38. Structure of the dicopper complex of 3,5-bis(11-hydroxy-undecanoxy) benzoate.

The procedure is summarized in Figure 42 below. A suspension was prepared with 3.0 g of the 3,5-bis(11-hydroxyundecanoxy) benzoic acid and 1.82 g triethylamine in 60 ml THF. A 1.45 mL aliquot of acryloyl chloride was added to this mixture. After over

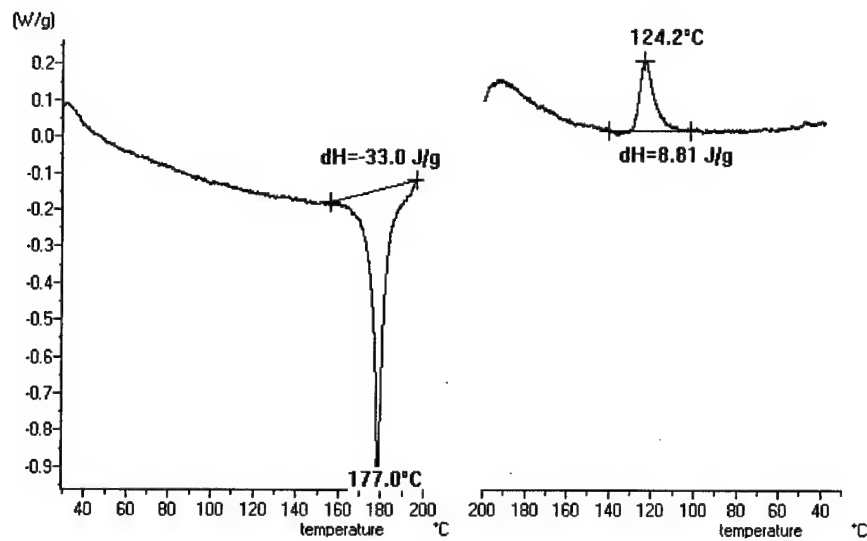


Figure 39. First DSC heating and cooling thermograms for of the dicopper complex of 3,5-bis(11-hydroxyundecanoxy)benzoate



Figure 40. Birefringence behavior of the dicopper complex of 3,5-bis(11-hydroxyundecanoxy)benzoate at 140 °C (under crossed polarization).

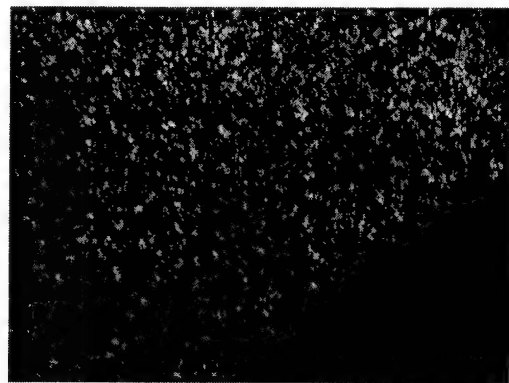


Figure 41. Birefringence behavior of the same dicopper complex of 3,5-bis(11-hydroxyundecanoxy)benzoate at 160 °C (under crossed polarization).

### 2.3.1.5 3,5-Bis(11-acryloyloxyundecanoxy)benzoic acid.

24 h stirring, THF was removed via rotovap and H<sub>2</sub>O was added. The final product of 3,5-bis(11-acryloyloxyundecanoxy) benzoic acid was extracted from H<sub>2</sub>O phase with chloroform. The chloroform solution was then washed with H<sub>2</sub>O for several times, dried with MgSO<sub>4</sub>, and evaporated to dryness. The crude product was finally purified by silica gel with CH<sub>2</sub>Cl<sub>2</sub> as eluent. Yield: 2.19 g (yellow oil).

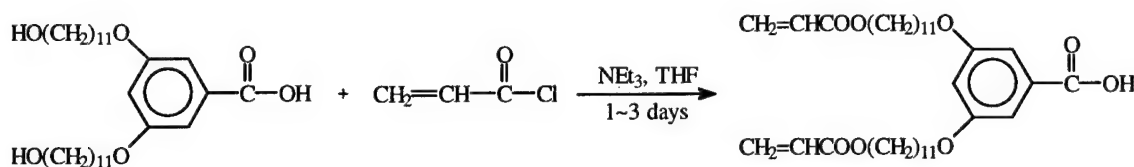


Figure 42. Synthesis of 3,5-bis(11-acryloyloxyundecanoxy) benzoic acid

#### 2.3.1.6. Copper 3,5-bis(11-acryloylundecanoxy) benzoate discotic LC thermoset.

The copper(II) complex of this monomer has been prepared from 3,5-bis(11-acryloyloxyundecanoxy) benzoic acid (see 2.3.1.5) by using a procedure similar to that provided in section 2.3.1.4. The monomer is a sticky semi-solid (gel) at room temperature. The DSC thermogram in Figure 44 clearly shows the discotic to isotropic

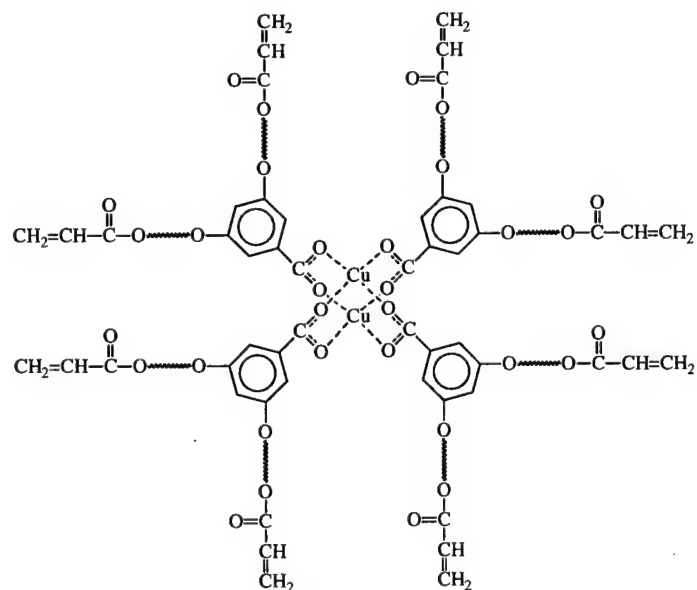


Figure 43. Structure of the Cu(II) complex of 3,5-bis(11-acryloylundecanoxy) benzoate.

transition temperature around 68 °C. Microscopy analysis showed very strong birefringence at temperature range from 40°C to 60°C. At 65°C, the birefringence disappeared slowly which is in agreement with the DSC results (Figure 45 a-e). About 20 grams of the acrylate LC thermoset with  $n=11$  was prepared and showed very good LC behavior.

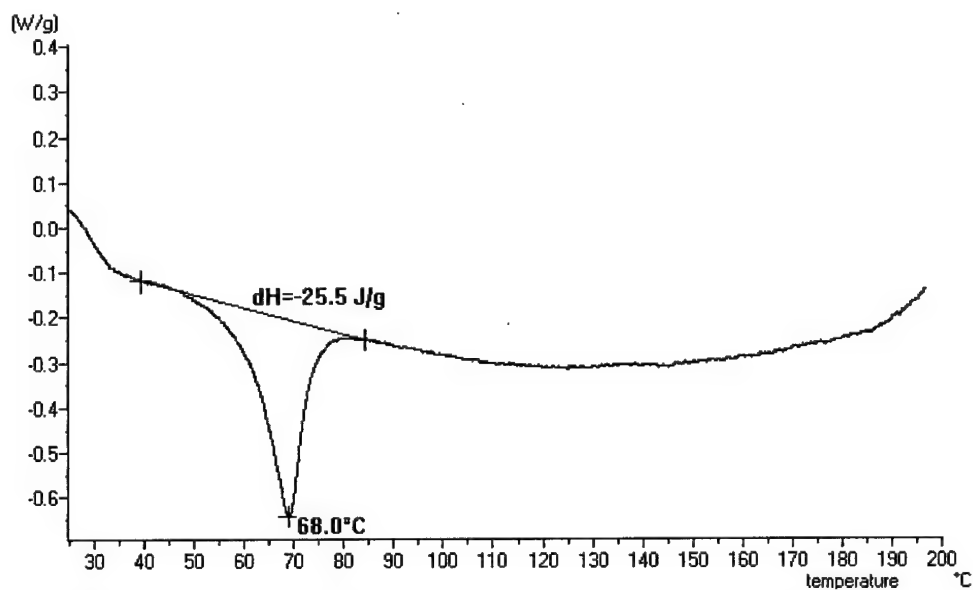


Figure 44. DSC analysis of the Cu(II) complex of 3,5-bis(11-acryloyl-undecanoxy)benzoate.

#### 2.3.1.7. Acrylate substituted discotic LC thermoset with $n=9$

The same procedure was used to prepare 7.6 grams of the acrylate substituted discotic monomer with a shorter flexible spacer ( $n=9$ ). Analysis of the solid by DSC indicated the discotic to isotropic phase transition temperature appeared at 49°C. Analysis of the solid using cross-polarized optical microscopy with a hot stage indicated that strong birefringence existed below the transition temperature and disappeared above.

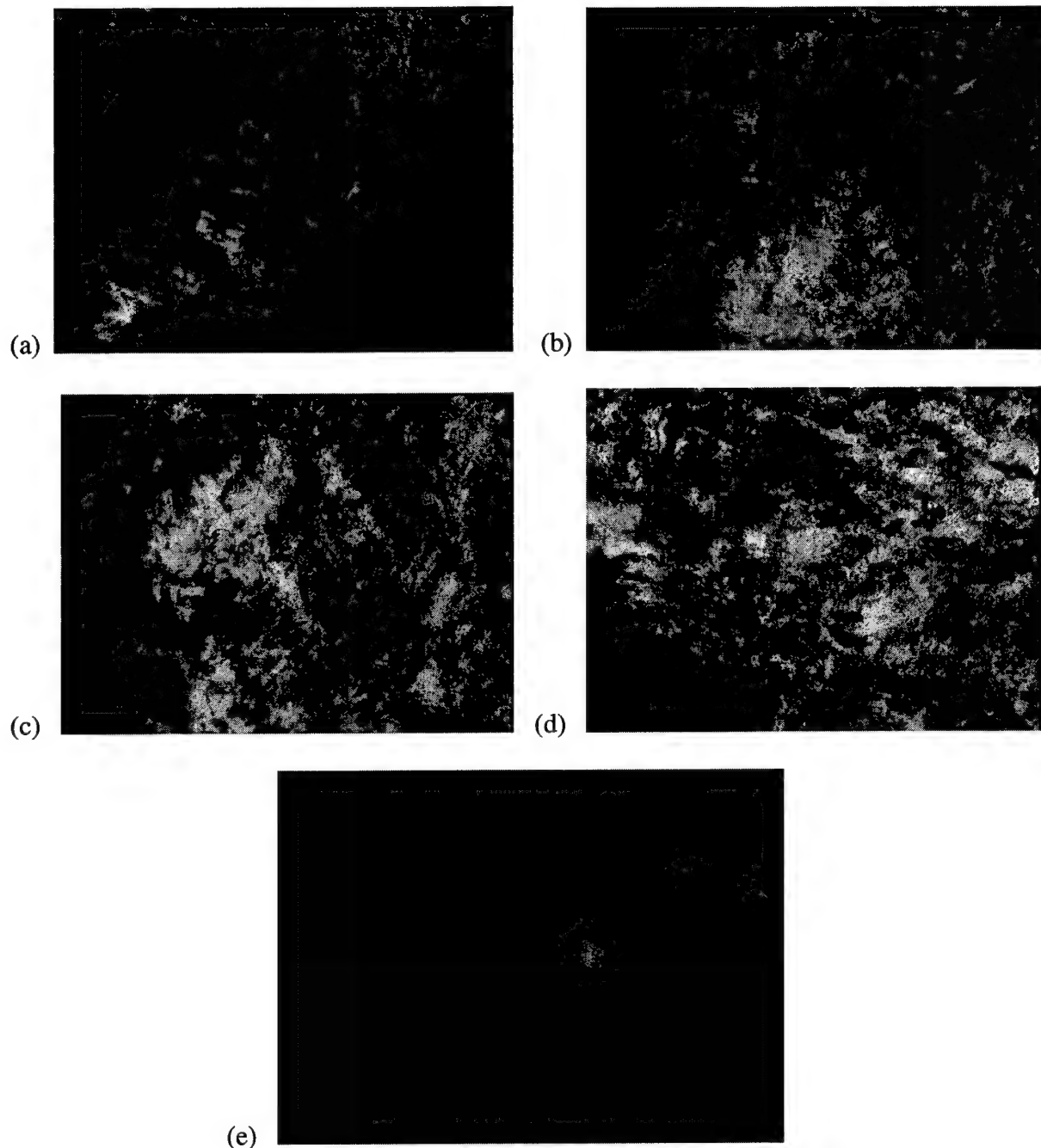


Figure 45. Hot stage microscope birefringence behavior of a thin film sample of the Cu(II) complex of 3,5-bis(11-acryloylundecanoxy) benzoate at different temperatures. Polarized transmitted light was used to illuminate the sample and a polarizer oriented perpendicular to the plane of the polarized transmitted light was placed on top of the sample. Temperatures for each view: (a) 40 °C, (b) 50 °C, (c) 55 °C, (d) 60 °C, (e) 65 °C

2.3.2. Discotic LC epoxy thermosets based on epoxy substituted benzoate complexes of Cu(II).

2.3.2.1. 3,5-Bis(11-dodecenenoxy)benzoate.

A procedure nearly identical to that described in sections 2.3.1.1 and 2.3.1.2 was used to generate the title compound, except that 12-bromodecene was used in place of the  $\alpha,\omega$ -bromoalcohol used previously. Figure 46 summarizes the procedures below.

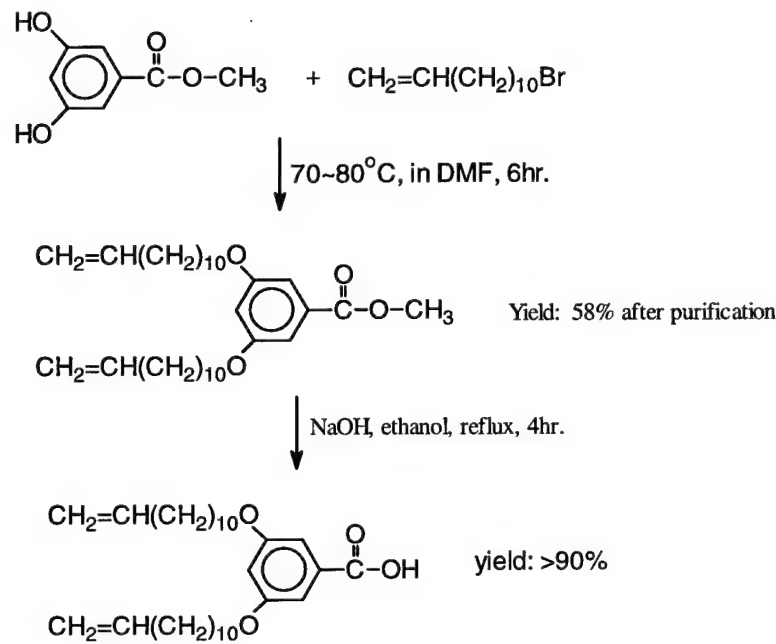


Figure 46. Synthesis of 3,5-bis(11-dodecenenoxy)benzoic acid

2.3.2.2. Epoxidation of 3,5-bis(11-dodecenenoxy)benzoate (n=10).

3, 5-Bis(11-dodecenenoxy)benzoic acid was epoxidized in the presence of 3-chloroperoxybenzoic acid utilizing a procedure based on that described in section 2.2.12 for the diketone mesogens. Starting from 4.6 gram of 3, 5-bis(11-dodecenenoxy)benzoic acid, 4.5 gram of the epoxidized product was obtained. The procedure is summarized in Figure 47 below.

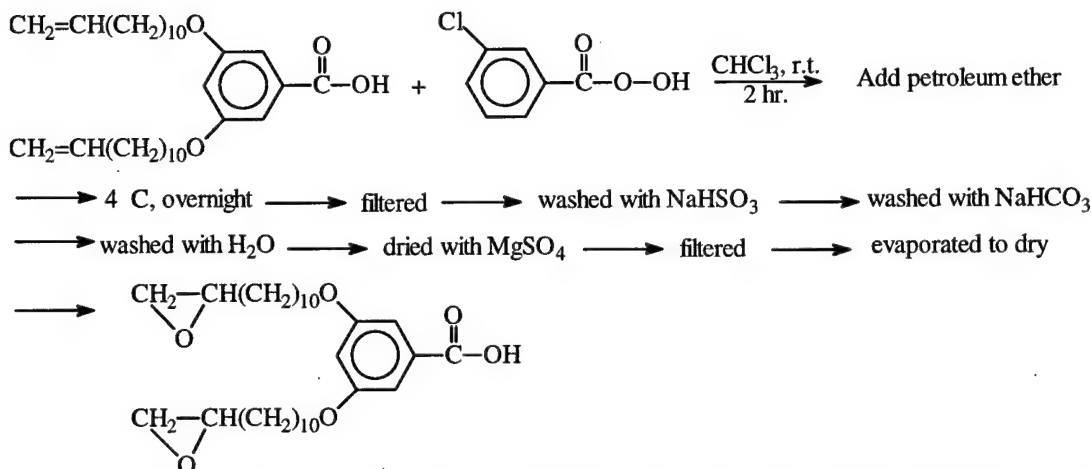


Figure 47. Synthetic procedure for epoxidation of the benzoic acid ligand with a  $n=10$  flexible chain length.

### 2.3.2.3. Epoxy LC thermoset resin based on the Cu(II) metallomesogen ( $n=10$ )

A 1.69 gram portion of the epoxy discotic LC thermoset was prepared from the material isolated in section 2.3.2.2 above via reaction with  $\text{Cu}(\text{OAc})_2$  in ethanol/water as described above. This is the final product in the synthetic pathway and the structure is shown below in Figure 48.  $^1\text{H}$  NMR analysis indicates that >80% of epoxide functionality was incorporated into the molecule relative to the initial alkene.

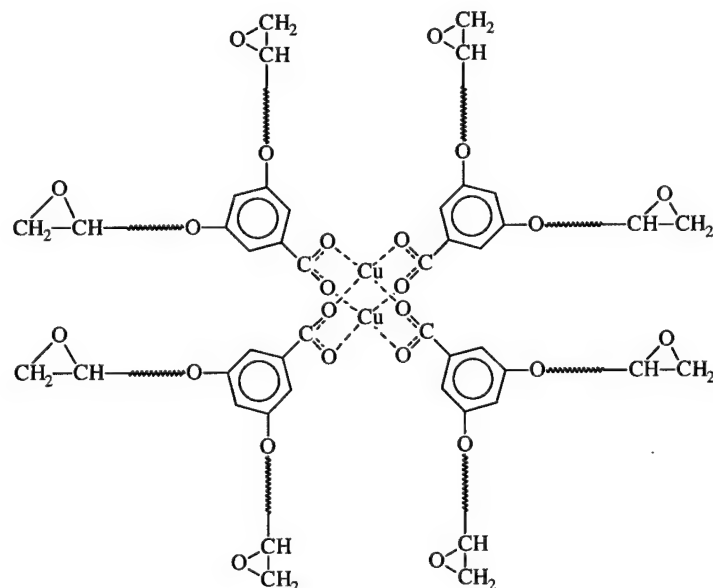


Figure 48. The structure of the prepared discotic LC epoxy.

Characterization of the epoxy thermoset material by DSC showed that the LC to isotropic phase transition occurred at 54 °C ( $\Delta H=12.3$  J/g). A thin film sample showed moderately strong birefringence at 40 °C, 45°C, 50 °C and 55 °C on a hot stage microscope. After 60 °C, the birefringence disappeared which was in agreement with DSC results. The birefringence images at various temperatures are shown in Figure 49.

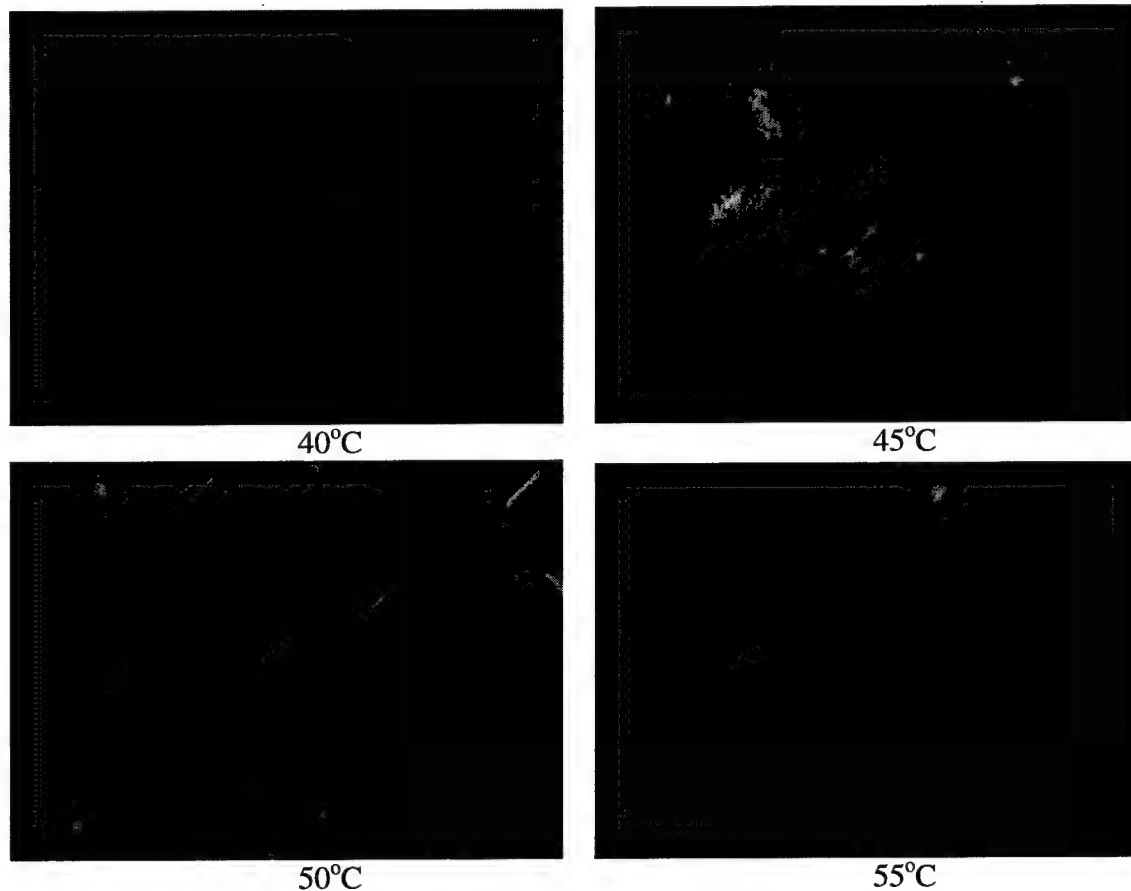


Figure 49. Birefringence images of discotic LC epoxy resin

#### 2.3.2.4. 8-Arm epoxy LC thermoset resin based on the Cu(II) metallocmesogen (n=9)

Due to the commercial availability of  $\text{CH}_2=\text{CH}(\text{CH}_2)_9\text{Br}$ , we decided to initiate the synthesis of the discotic LC epoxy resins with n=9 in the flexible spacer group. Using the same approach described in sections above, about 12.7 g of thermoset resin was obtained with >80% epoxy functionality relative to the initial vinyl group concentration.

The discotic LC to isotropic phase transition temperature was identified by DSC results (Figure 50) to be 69.8°C (heating rate 10°C/min).

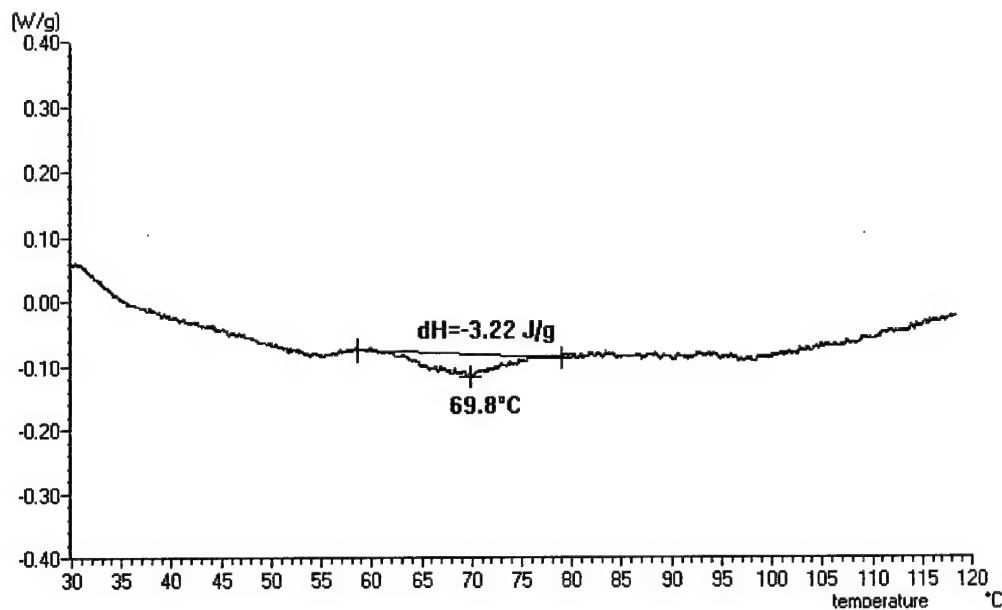


Figure 50. First DSC heating thermogram of the n=9 discotic LC epoxy complex. Heating rate: 10 °C.

Strong birefringence was observed at 40, 50, and 60°C and weaker at 70°C.

#### 2.3.2.5. 4-Arm acrylate LC thermoset resin based on Cu(II) metallomesogens (n=9)

The previous four thermoset monomers described in preceding sections showed very promising LC behavior but a relatively low LC transition temperature. In order to increase the transition temperature, we initiated two new approaches: 1) reduce the flexible space length "n"; and 2) use only one flexible substituent per benzene ring.

The monomer structure and synthesis procedure are illustrated in Figure 51. About 6 grams of the monomer were prepared using the standard methods described earlier and characterized by DSC and optical microscopy. When the material was analyzed by DSC, no transition peaks were observed in the range of room temperature to 180 °C. However, the crosslinking peak (homopolymerization of the acrylate resin) was observed to start

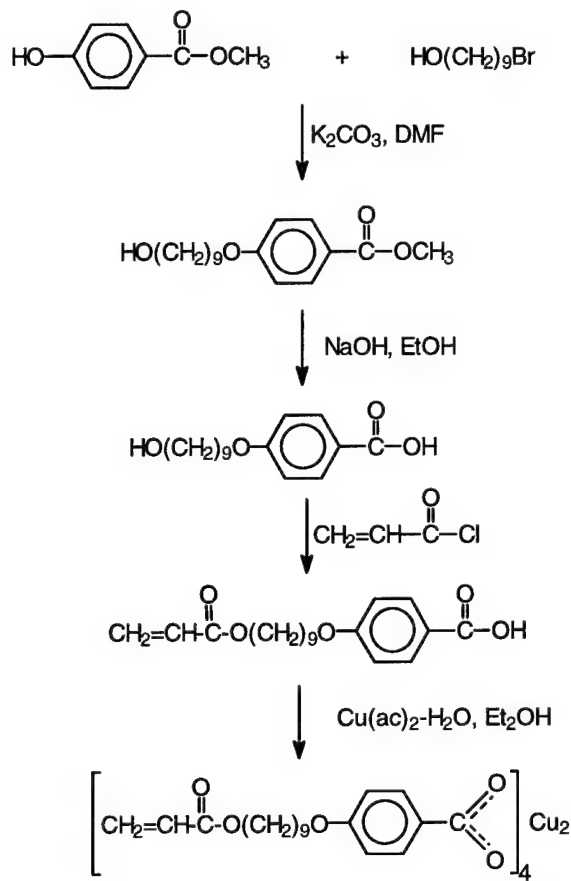


Figure 51. Synthetic pathway to a new discotic LC monomer with higher transition temperature

around 170 °C. Polarized optical microscopy analysis indicated the presence of very strong birefringence from room temperature to 180 °C. The monomer was solid at room temperature and started floating freely (viscous liquid) after reaching 120 °C. It is very likely that the LC to isotropic phase transition temperature is higher than the thermal crosslinking temperature.

We synthesized small quantities of the Co(II), Zn(II) and Ni(II) analogues of the Cu(II) n=9 discotic LC acrylate resin. We were surprised to discover that none of these new resins demonstrated any birefringence. As a result, we confined our subsequent investigations to the Cu(II) complexes.

### 2.3.2.6. 8-Arm epoxy LC thermoset resin based on Cu(II) metallomesogen (n=4)

As discussed in the preceding section, the discotic to isotropic phase transition temperature for the tetraacrylate resin was higher than the thermal curing temperature for the metallomesogen with four flexible spacer arms. A second approach to raising the LC transition temperature is to shorten the length of the flexible spacer on the 8-arm resins to n=4. In order to accomplish this important goal, we needed to synthesize 6-bromo-1-hexene, alkylate the hydroxyl positions, and finally epoxidize the pendant alkene groups to generate the 8-arm epoxy product. The  $\text{CH}_2=\text{CH}(\text{CH}_2)_4\text{Br}$  was prepared by the method illustrated in Figure 52 starting with  $\text{Br}(\text{CH}_2)_6\text{Br}$ .

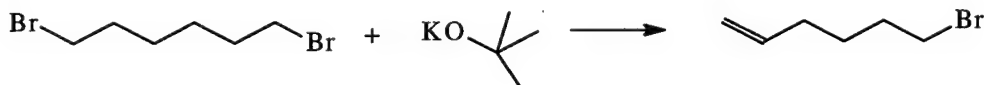


Figure 52. Preparation of 6-bromo-1-hexene for use in synthesizing discotic LC epoxy resins with shorter flexible spacers (for raising LC transition temperatures).

To a mixture of 200 g 1,6-dibromohexane and 125 ml tetrohydrofuran(THF) is added (with stirring and cooling the flask in an ice-bath) a solution of 113 g of potassium t-butoxide in 425 ml THF over a period of 45 minutes. The temperature was maintained between 25 – 30 °C. The reaction mixture was refluxed for 30 minutes, followed by removal of low boiling ingredients (THF and hexadiene) using a rotary evaporator. Subsequently, the t-BuOH side-product was distilled off at atmospheric pressure. The  $\text{CH}_2=\text{CH}(\text{CH}_2)_4\text{Br}$  was then distilled from the reaction residue at reduced pressure and collected as a colorless liquid. b.p. 100-105°C/~100mmHg. Yield 51 g.

The alkylation of (3,5-dihydroxy)methylbenzoate and subsequent reaction chemistry to generate the acid, octaepoxy derivative and finally the Cu(II) complex was carried out using procedures illustrated in Figure 53 and described in detail in preceding sections.

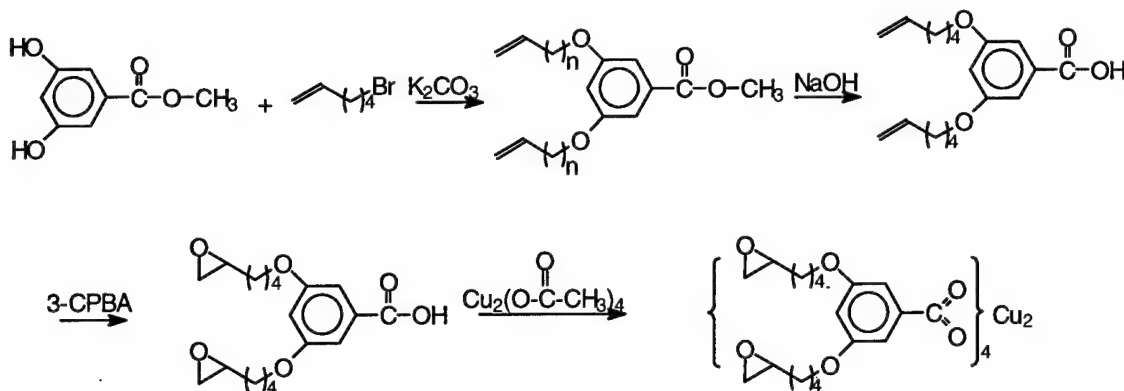


Figure 53. Synthetic pathway to the short flexible spacer ( $n=4$ ) 8-arm discotic LC epoxy monomer.

The structure of the discotic LC epoxy monomer with the  $n=4$  pendant spacer groups is shown in Figure 54 below. About 10 grams of the material were obtained. The  $n=4$ , 8-arm discotic LC epoxy resin was analyzed by DSC, and showed two distinct endotherms at 94 and 141 °C respectively (Figure 55). This confirmed that the LC transition was indeed moved to a higher temperature (relative to  $n=9$  or higher) by shortening the flexible spacer arms to  $n=4$ .

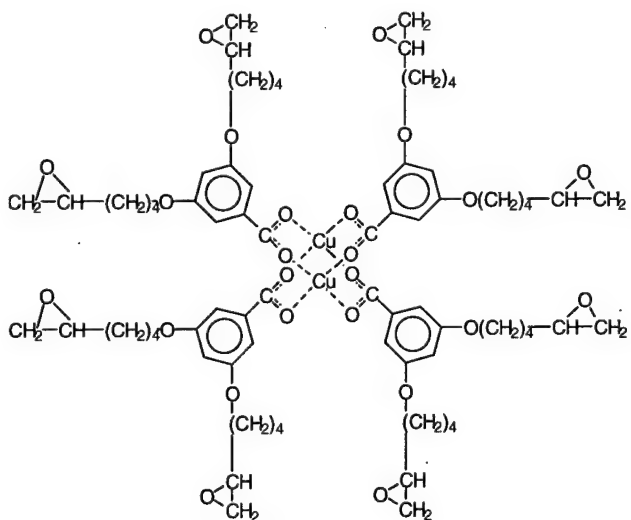


Figure 54. Structure of the discotic LC epoxy monomer with shorter flexible spacer arms ( $n=4$ ) intended to give a higher LC transition temperature compared to the previous longer chained resins.

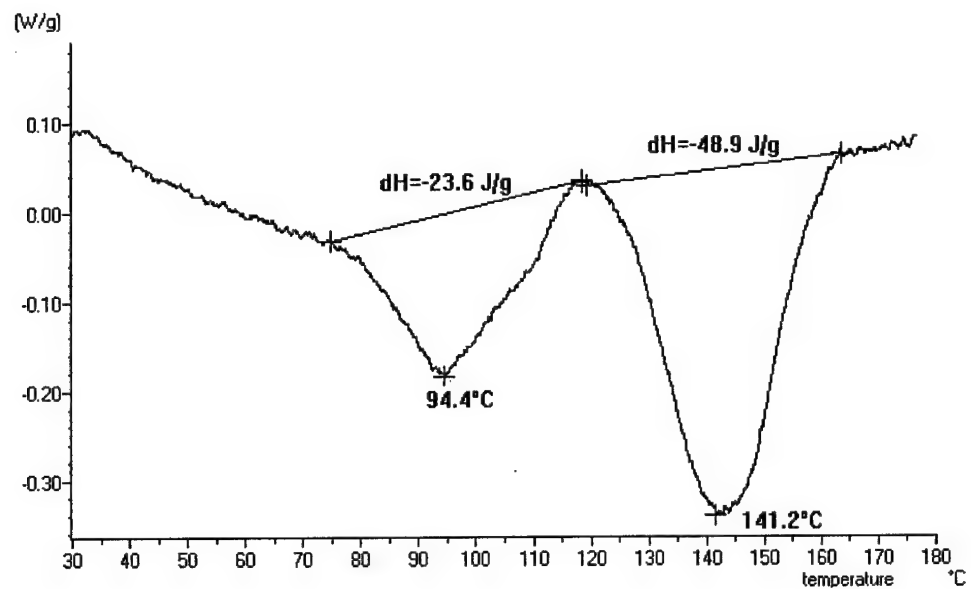


Figure 55. DSC thermogram for  $n=4$ , 8-arm discotic LC epoxy monomer. The peak at  $94\text{ }^{\circ}\text{C}$  is assigned to the crystalline to discotic phase transition ( $\text{K} \rightarrow \text{N}_d$ ) and the larger endothermic peak at  $141\text{ }^{\circ}\text{C}$  is assigned to the discotic to isotropic melting transition ( $\text{N}_d \rightarrow \text{I}$ ).

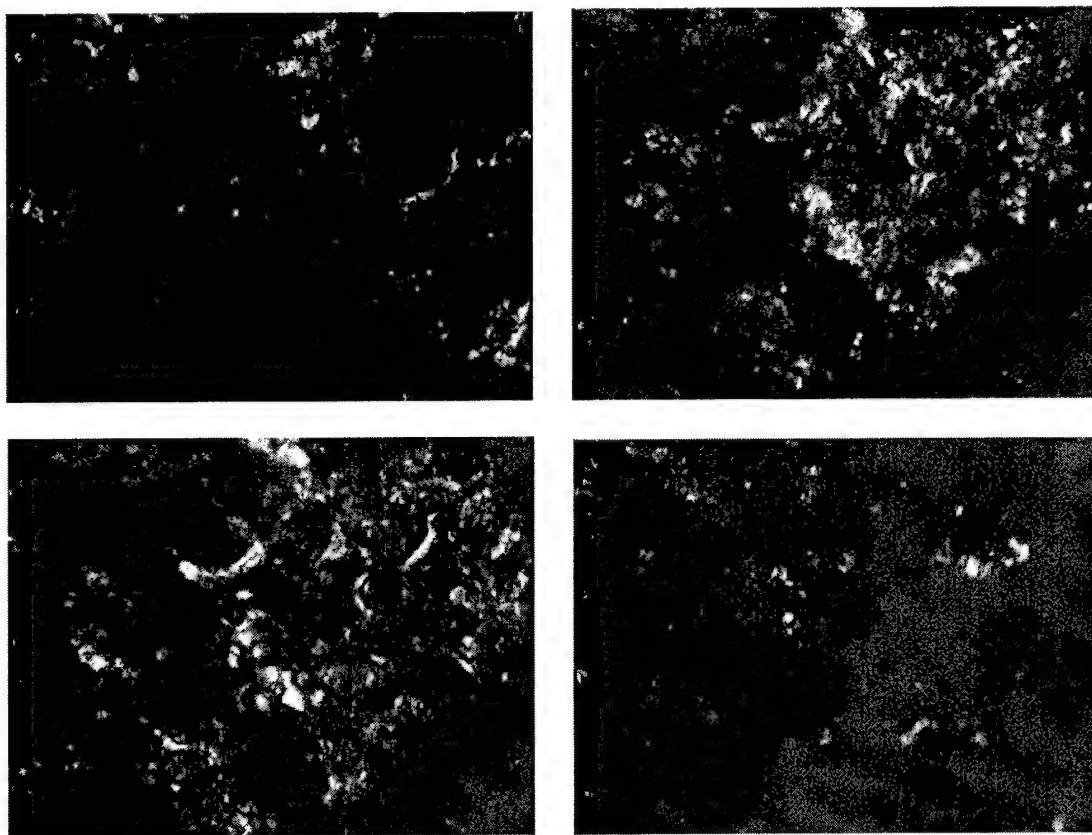


Figure 56. Polarized optical microscopy of the  $n=4$ , 8-arm discotic LC epoxy resin.

The new monomer was also analyzed by polarized optical microscopy as a function of temperature. The material showed strong birefringence at room temperatures and continued this behavior at elevated temperatures as shown in Figure 56.

### 2.3.2.7. Summary of discotic LC resins based on the 8-arm mesogenic core

In order to expand the availability of discotic LC monomers, we also synthesized epoxy monomers with a flexible spacer length of  $n=6$ . The starting material 8-bromo-1-octene was prepared from 1,8-dibromoocetane in ~40% yield by using the previously established procedure for 6-bromo-1-hexene. By following the procedure described above, more than 10 grams of the epoxy thermoset monomer with  $n=6$  was isolated. The prepared discotic LC epoxy will be analyzed by DSC and optical microscopy. Table 1 summarizes some pertinent information on the family of 8-arm discotic LC epoxy monomers.

Table 1. New thermoset monomers with discotic LC characteristics based on metallomesogens.

Monomer	n	M	$T_{d \rightarrow l} (^\circ C)$	$\Delta H_{d \rightarrow l} (J/g)$	Birefringence
Acrylate	9	Cu	49	15.0	Very strong
Acrylate	11	Cu	68	25.5	Very strong
Epoxy	10	Cu	54	12.3	medium
Epoxy	9	Cu	70	3.34	strong
Epoxy	9	Co	none	-	little
Epoxy	9	Zn	none	-	little
Epoxy	9	Ni	none	-	little
Epoxy	4	Cu	141	48.9	Strong
Epoxy	6	Cu	broad		strong

## 2.4 Discotic LC resin curing chemistry

### 2.4.1 Acrylate Substituted Monomers.

Since the transition temperature observed is below 80 °C, we initially believed that it would be unlikely that conventional thermal free-radical reactions can be used to cure the monomer. However, when the discotic acrylate LC monomer with  $n=11$  was heated at 100 °C for 2 hours in the presence of 2 wt% of AIBN, the fully cured sample (surprisingly) showed strong birefringence (Figure 57). However, the film was very brittle.

Even though the curing temperature was much higher than  $T_{d \rightarrow I}$ , the cured sample maintained a significant degree of ordered LC domains, and therefore, free radical induced cross-linking is an efficient curing method for the  $n=11$  discotic acrylate monomer.

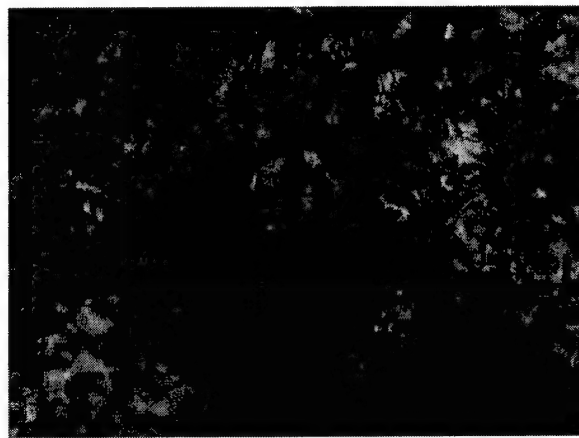


Figure 57. After free radical curing above the isotropic clearing temperature, the discotic LC acrylate ( $n=11$ ) thermoset resin still shows crystalline order.

High energy photons (ultra-violet and visible) can be used as curing source with/without free-radical photo-initiators. High energy photon curing (brief exposure to an unfiltered 250 W medium pressure mercury arc lamp (Oriel)) was tried for the acrylate monomer with  $n=11$  without a photo-initiator at room temperature. Partial curing was

observed. Previously, photocuring of discotic acrylate LC monomer in the absence of photo-initiator had been tried. No substantial curing was observed after the sample irradiated under high-energy photon. When another sample of the  $n=11$  monomer was mixed with 1 wt% of 2,2-dimethoxy-2-phenylacetophenone (a potent photoinitiator) and heated to 45 °C under the same UV-curing conditions, no difference was noted even after an hour.

#### 2.4.2 Epoxy Substituted Monomers.

The epoxy monomer ( $n=9$ ) was mixed with polyamine (diethylene triamine) in THF and a solvent cast was made (Figure 58). The curing reaction was allowed to proceed at room temperature. A typical procedure for making a thin polymer film via solvent casting is shown below.

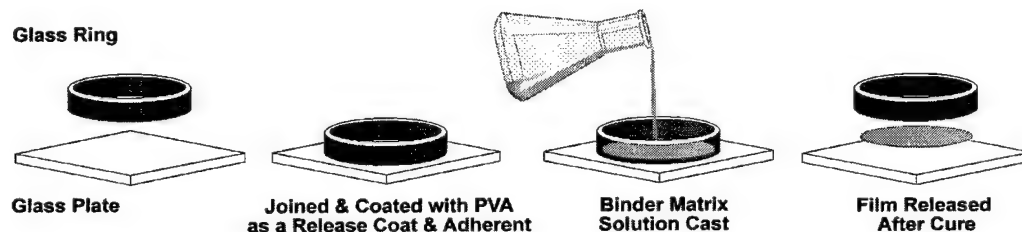


Figure 58. Solvent casting method used to make thin thermoset polymer films from discotic LC epoxy resins and polyfunctional amine curing agents.

The cast film was monitored by polarized optical microscopy daily or weekly (depending on the curing rate progression). A typical set of observations for the  $n=9$  compound mixed with diethylenetriamine and cast in THF into the mold are as follows:

- 3 days: many bubbles in the film. Degassed under vacuum for about 10 minutes.
- 4 days: observed very few spots of birefringence.
- 5 days: same as day 4. Bubbles still present; degassed overnight in vacuum.
- 6 to 8 days: no substantial change under microscopy. Film loses tack.
- 30 days: film was released from the glass plate and a flexible film was obtained which showed some birefringence under polarized microscopy.

A 30-day curing cycle at room temperature was selected based on literature precedents (Shell Chemical Co., Tech. Bulls. SP-23A, SP-24B and SP-24C; "Epoxy Resin Technology", 2<sup>nd</sup> Ed., Edited by Clayton A. May, Marcel Dekker, Inc.: New York, 1988, p519).

The n=4, 8-arm epoxy resin described in section 2.3.2.6 was similarly cured using diethylenetriamine as the curing agent and THF as the solvent. After mixing the miscible viscous liquid mixture showed strong birefringence under cross-polarization (Figure 59).

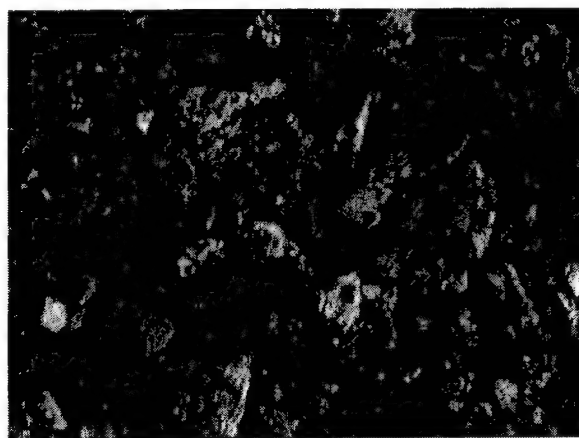


Figure 59. Discotic LC epoxy monomer (n=4) mixed with diethylenetriamine in THF at room temperature.

#### 2.4.2.1. Polyamine Curing Agents

In order to optimize the mechanical properties of the cured samples, we screened different polyamines (both aliphatic and aromatic) of variable molecular weight and functional group density. The structures of polyamines chosen are given in Figure 60.

#### 2.4.2.2. Curing of the 8-arm discotic LC epoxy with n=4

Based on the promising results for the n=4 epoxy curing with diethylenetriamine described above, we decided to screen aliphatic polyamines for curing conditions that retained a significant degree of LC behavior (determined by observation of substantial birefringence in cross-polarized optical microscopy). Preliminary testing ruled out using

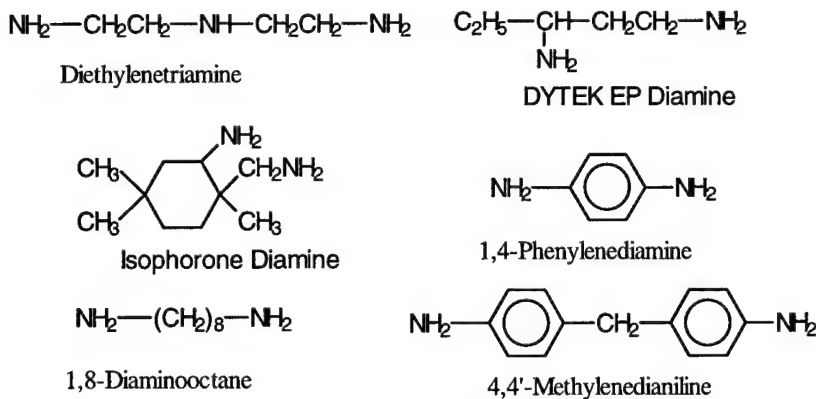


Figure 60. Polyamines used for discotic LC epoxy curing

aromatic diamines (stiff) with the shorter, less flexible  $n=4$ , 8-arm discotic LC resin. The results are summarized in Table 2. Unfortunately, the mechanical properties of the resulting cured film are very dependent on the structure of the amine curing agent, and only diethylenetriamine gave a film with satisfactory strength.

Table 2. Fabrication of samples with discotic liquid crystal epoxy ( $n=4$ )

Curing Agent	Curing Condition	Results
Diethylenetriamine	100°C, 4 hours	<b>Strong, Semi-Flexible Film</b>
1,8-Diaminoctane	Room Temperature	Crack
1,4-Phenylenediamine	100°C, 24 hours	Crack
Isophorone Diamine	100°C, 6 hours	Brittle Film
4,4'-Methylenedianiline	100°C, 6 hours	Brittle Film

#### 2.4.2.3. Curing of the 8-arm discotic LC epoxy with $n=9$

A similar strategy to that described in the preceding section was undertaken with the  $n=9$ , 8-arm epoxy. The results are summarized in Table 3.

The results in Tables 2 and 3 indicate that discotic liquid crystal thermoset epoxies with either long or short pendant, flexible spacer arms can be fabricated into a film with desirable mechanical properties. The selection of polyamine is obviously critical for different discotic liquid crystal monomers.

Table 3. Fabrication of samples with discotic liquid crystal epoxy (n=9)

Curing Agent	Curing Condition	Results
Diethylenetriamine	80°C, 2.5 hours	Flexible Film
1,8-Diaminoctane	80°C, 2.5 hours	Flexible Film
1,4-Phenylenediamine	100°C, 24 hours	Brittle Film
Isophorone Diamine	80°C, 2.5 hours	Brittle Film
DYTEK EP Diamine	80°C, 2.5 hours	Flexible Film
4,4'-Methylenedianiline	80°C, 2.5 hours	<b>Semi-Flexible, Strong Film</b>

#### 2.4.2.4. Curing of a new 4-arm discotic LC epoxy with n=9

We designed and prepared a new discotic liquid crystal thermoset monomer with the structure shown in Figure 61. Unlike the previous thermoset monomers, this new monomer has only 4 flexible arms (instead of 8) with a medium spacer length of n=9. It was observed that the LC phase of this discotic LC monomer can be maintained after the monomer was cured with certain polyamines.

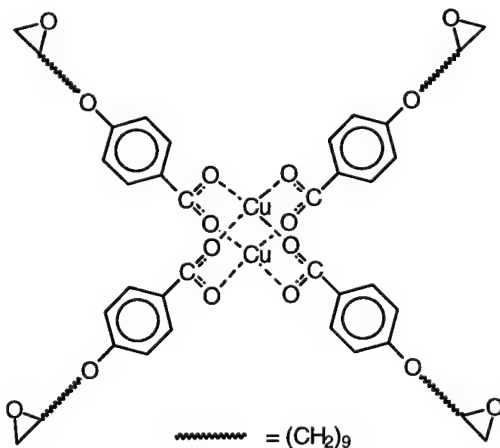


Figure 61. Structure of the discotic liquid crystal epoxy thermoset monomer (n=9).

The new monomer, as shown in Figure 61, was prepared by using the procedure illustrated in Figure 62, and analogous to those described in detail previously. An important modification to the epoxidation procedure was to run the reaction for 24 hours instead of only 2 hours, *thus giving a higher degree of epoxide incorporation into the*

*monomer.* This in turn leads to a more pure monomer, with a higher LC transition temperature and more desirable mechanical properties on curing with polyamines.

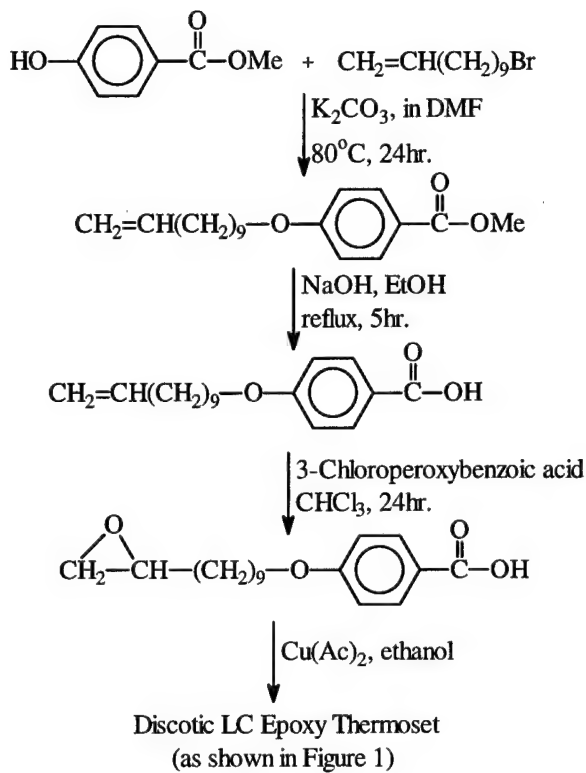


Figure 62. Synthetic procedure (modified) for the synthesis of the improved 4-arm,  $n=9$  discotic LC epoxy resin.

The prepared monomer was analyzed by DSC (Figure 63). During the first heating scan (30 to  $200^\circ\text{C}$ ,  $10^\circ\text{C}/\text{min}$ ), a endothermic melting peak was observed at  $98.6^\circ\text{C}$  with a heat of fusion  $\Delta H$   $58.5 \text{ J/g}$ . The exothermic peak at  $193.6^\circ\text{C}$  corresponds to the homopolymerization curing of the epoxy monomer. Strong birefringence was observed by cross-polarized microscopy at room temperature and above.

The new monomer was cured with a variety of diamines similar to those given in Figure 60. Specifically, 0.5 g of monomer was dissolved in 5 ml of THF to obtain a viscous homogeneous solution. In this solution, a stoichiometric quantity of polyamine (based on the number of NH per epoxy) was added. The solution was poured into a

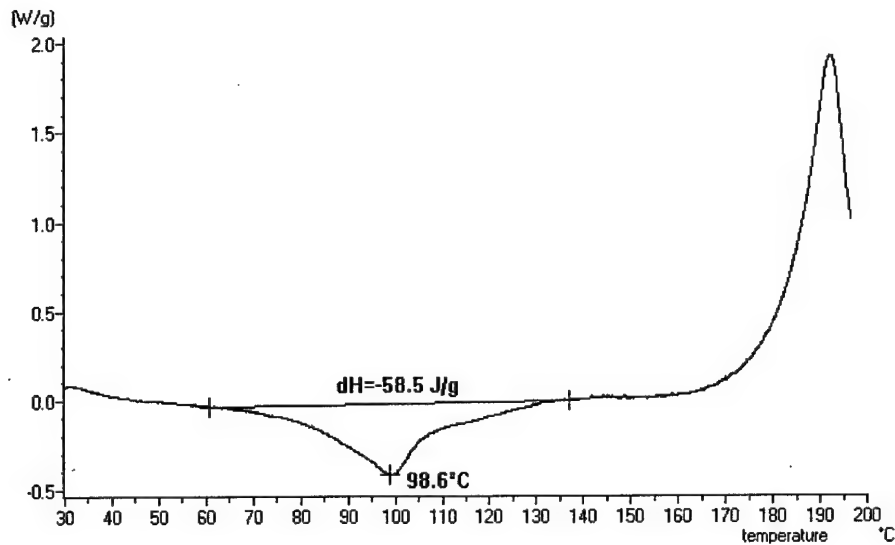


Figure 63. DSC thermogram of 4-armed,  $n=9$  discotic LC epoxy.

releasing-agent treated aluminum weighting boat. The solvent was then evaporated slowly. After the complete evaporation of solvent, the thermoset film was obtained and analyzed by microscopy to check the LC phase. The preliminary results are summarized in Table 4.

Table 4. Discotic liquid crystal epoxy thermoset (4-arm,  $n=9$ ) curing with amines.

Polyamine	Film	LC Phase
Diethylenetriamine	Very Strong	Weak
1,3-Diaminopropane	Semi-Brittle	<b>Very Strong</b>
1,4-Phenylenediamine	Brittle	Little
Isophorone Diamine	Crack	<b>Strong</b>
DYTEK EP Diamine	Very Strong	No
4,4'-Methylenedianiline	brittle	No

The film obtained by curing with 1,3-diaminopropane was particularly bright under the cross-polarization conditions, indicating a high degree of birefringence and crystalline order.

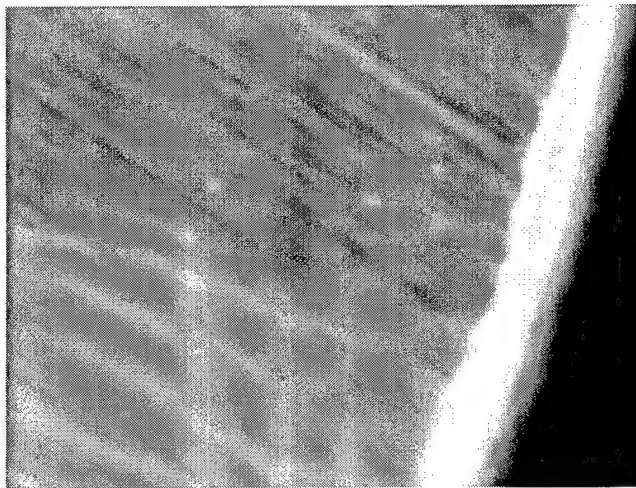


Figure 64. Cross-polarized microscopic view of film from 4-arm, n=9 discotic LC epoxy monomer cured with 1,3-diaminopropane at room temperature.

#### 2.4.2.5. Curing of blends of 4-arm and 8-arm discotic LC epoxy with n=9

Mixtures of 4-arm and 8-arm discotic LC epoxies (see Figure 3) were formulated with 1, 3-diaminopropane and cured at room temperature in an attempt to extend the mechanical properties and curing conditions of the new discotic LC epoxy resins. The results are summarized in Table 5.

Table 5. Discotic LC epoxy mixtures cured with 1,3-diaminopropane at room temp.

4-arm monomer	8-arm monomer	LC Phase <sup>1</sup>	LC Phase <sup>2</sup>
20%	80%	Yes	No
40%	60%	Yes	no
60%	40%	Strong	Weak
80%	20%	Very strong	Strong

<sup>1</sup>room temperature curing after 1 week;

<sup>2</sup>room temperature curing for 1 week and 100°C curing for 3 hours.

After 2 weeks of room temperature curing, LC phases were observed for all of these formulations. As expected, the flexibility of the cured film increased with increasing the percentage of 8-arm discotic monomers. However, since the monomers were not completely soluble, the films prepared were not always homogeneous. We found that

blending pre-made solutions of each discotic LC epoxy first and then mixing them gave homogeneous solutions and thermoset films. After about one week of room temperature curing, all the films showed birefringence under cross-polarized microscopy. Then the films were cured at 100°C for 3 hours. We found that after 100°C curing procedure , only the thermoset film with high percentage of 4-arm monomer showed strong LC phase, as shown in Figure 65. DSC analysis showed the film was not completely cured however.

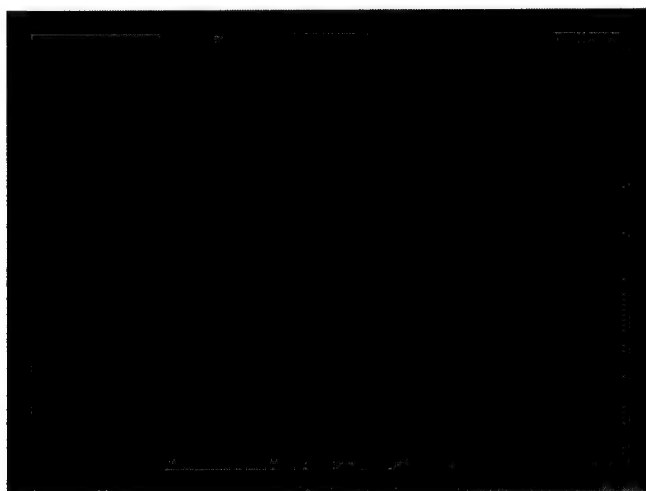


Figure 65. LC phase observed in film of 80% 4-arm monomer and 20% 8-arm monomer cured with 1,3-propanediamine at room temperature (1 week) followed by a post-cure anneal at 100 °C (3 hours).

A second promising formulation was discovered using a 2:3 ratio of 8-arm : 4-arm discotic epoxy monomers and 1,3-propane diamine as the curing agent. The film was cured at room temperature for 2 weeks, followed by heating at 50 °C for 20 hours and then at 65 °C for an additional 24 hours. The film was cured according to DSC analysis and showed reasonable strength and flexibility. Figures 66(a) and (b) show the resulting birefringence images for this blend after room temperature curing and after the 50 °C annealing period.

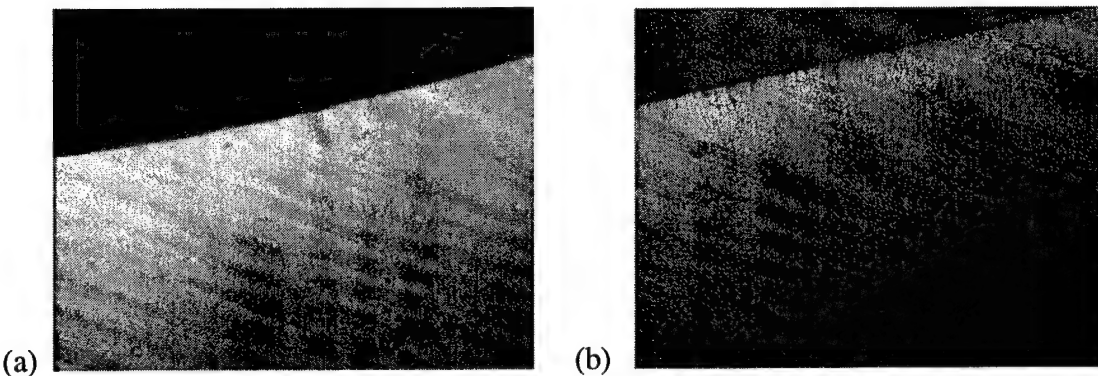


Figure 66. Birefringence images of 4-arm/8-arm discotic blending systems (a) after room temperature curing and (b) after 50°C curing.

#### 2.4.2.6. Curing of blends of 4-arm discotic LC epoxy resin with aliphatic LC epoxy resins for increased film flexibility and toughness.

To investigate the effect of adding a more flexible co-reactant to the 4-arm epoxy matrix, we synthesized an aliphatic discotic LC epoxy as shown in Figure 67. We anticipated that this monomer would increase the flexibility of the formulated films if added in small quantities without destroying the LC phase, and this appeared to be born out by experiment (Table 6). DSC analysis of this monomer showed a strong endothermic peak during the first heating scan from 30 to 150°C at 10°C/min.  $T_m = 110^\circ\text{C}$ ;  $\Delta H = 66 \text{ J/g}$ .

Table 6. Aliphatic discotic epoxy blends with 4-arm ( $n=9$ ) discotic LC epoxy cured with 1,3-propanediamine at room temperature.

Sample	Weight ratio of 4-arm/aliphatic	Birefringence
1	9/1	Strong
2	8/2	Strong
3	7/3	Strong
4	0/1	Weak

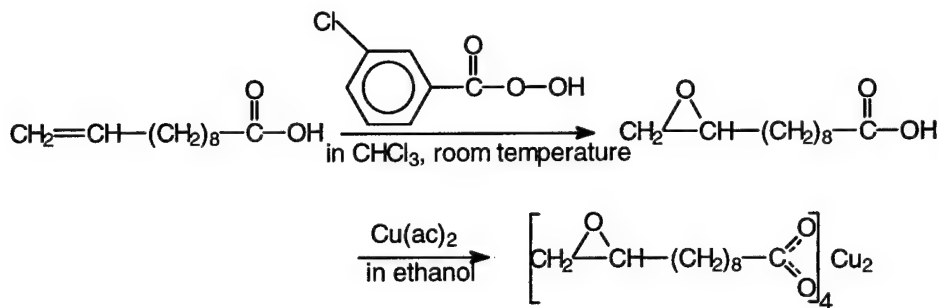


Figure 67. Synthetic pathway to the aliphatic discotic epoxy co-monomer

The blended samples appeared to have very strong birefringence after curing for 4 days at room temperature (Figure 68). The birefringence was undiminished after curing for a month at room temperature followed by a post-cure anneal at 100 °C for 3 hours.

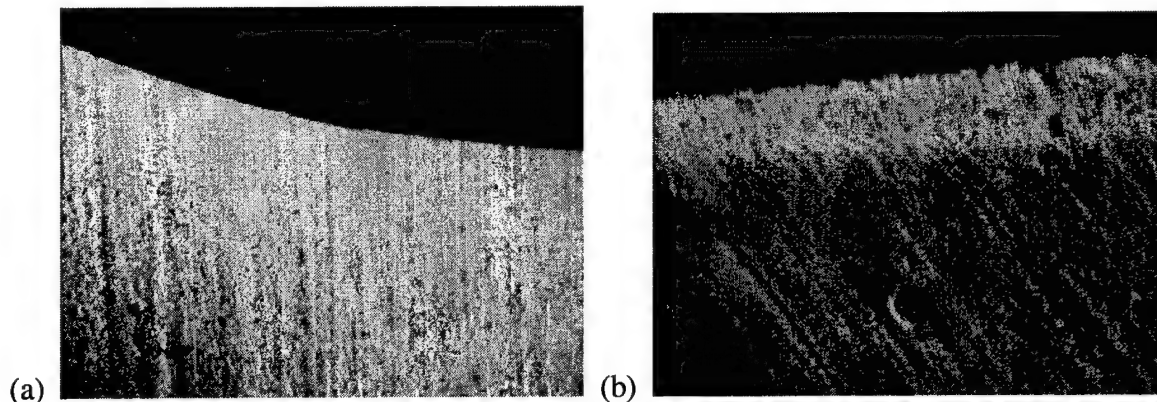


Figure 68. (a) Sample 1 and (b) sample 2 from Table 7 above. The films were cured for four days at room temperature when these birefringence images were taken.

## 2.5 Summary of synthesis, isolation and curing of discotic LC thermoset resins

Of the candidate resins for highly conductive, discotic LC thermoset materials described up to now, the benzoate systems appear to have the most promise from a synthetic economy and physical performance point of view. We have demonstrated a large variety of conditions that yield cross-linked thermoset matrices which retain LC character based on these novel discotic Cu(II) mesogenic resins. Using the procedures

described in this report, the new resins would still be too costly however for large scale applications as commodity matrix materials.

The goals of this research project were:

- Develop synthetic routes to a series of epoxy modified discotic liquid crystalline thermoset monomers.
- Demonstrate monomer curing via cross-linking co-reactants, while retaining Z-directional orientation.
- Assess physical properties of thermally conductive polymer matrices.
- Test thermal conductivity of cured materials.

In the next section we will discuss the thermal conductivity of the most promising resins (those that have enough mechanical stability to be handled without breaking).

### 3.1. Thermal conductivity Testing Methods

Thermal diffusivity and specific heat of the samples were measured at 100 °C by the laser flash method utilizing a Holometrix Microflash instrument. This instrument and method conform to ASTM E1461-92, "Standard Test Method for Thermal Diffusivity of Solids by the Flash Method" for the measurement of thermal diffusivity. The measured values of thickness, bulk density, specific heat, thermal diffusivity and the calculated thermal conductivity have not been corrected for thermal expansion. The samples were coated with approximately 0.1  $\mu\text{m}$  of gold and 5  $\mu\text{m}$  of graphite for testing. Due to non-uniform sample thickness, the measurement uncertainties are higher than normal. The diffusivity and specific heat values are estimated to be accurate to within  $\pm 10\%$ , the bulk density values within  $\pm 8\%$  and the calculated conductivity values within  $\pm 15\%$ .

### 3.2 Thermal conductivity results for cured discotic LC resins

Two of the 8-arm, discotic LC epoxy samples cured with 1,3-propanediamine (see section 2 above) were analyzed by Holometrix, Inc. for evaluation of the thermal conductivity according to the ASTM E1461-92 flash diffusivity method. The results are summarized in Table 7.

Table 7. Thermal conductivity results for the 8-arm, discotic LC epoxies with n=4 and n=9 flexible spacer chain lengths cured with 1,3-propanediamine.

Sample	Method	Conductivity (W/mK)
LC Epoxy (n=4)	ASTM 1461-92	0.30
LC Epoxy (n=9)	ASTM 1461-92	0.24
Polyurethane/Alumina(9/1)	Literature Data	0.122~0.125
Polyurethane/Carbon Fiber(9/1)	Literature Data	0.41

The results obtained above were disappointing, in that the thermal conductivity values are only nominally better than standard resin matrices.. The birefringence of the two samples was not very intense, but the films had flexibility and mechanical strength suitable for small samples to be cut from them for testing without fracturing. We believed that testing the best samples we could obtain, based on the intensity of the birefringence and the mechanical stability of the films, would be the crucial factor to determine whether it is possible to obtain highly conductive cured epoxy matrices using the discotic metallomesogen approach undertaken as the focus of this project. The discotic 4-arm/8-arm blend and the discotic 4-arm/aliphatic epoxy blend samples described in detail above were cured with 1,3-propanediamine and measured using the Holometrix method. For a more complete comparison, a thin film sample of standard bis-phenol A epoxy resin (Epon-828<sup>®</sup>, Shell Chemical) cured with 1,3-propanediamine was also measured using the same method, as well as a highly oriented sample of a rod-

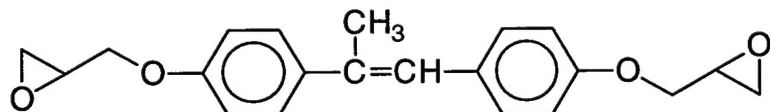


Figure 69. DHAMS, the diglycidyl ether of dihydroxy- $\alpha$ -methylstilbene

like LC mesogen resin, the diglycidyl ether of dihydroxy- $\alpha$ -methylstilbene (DHAMS, Figure 69). The DHAMS resin, synthesized economically in a two-step process from phenol, chloroacetone, sulfuric acid and epichlorohydrin, is available in experimental quantities from Dow Chemical Company. DHAMS was cured in the smectic phase with bis(4-aminophenyl)disulfone (DADS) at 80 °C for 2 hours followed by a 2 hour post-cure at 125 °C. The sample was very birefringent (Figure 70), indicating a high degree of molecular alignment. The thermal conductivity results and other physical property measurements are give in Table 8 for the two previously mentioned samples (Table 7) as well as the new samples.

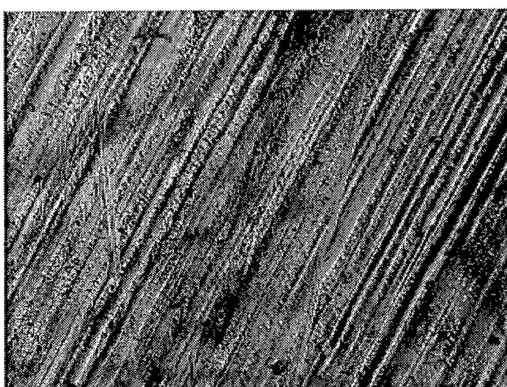


Figure 70. Birefringence image of a film of DHAMS cured with DADS in the smectic LC state.

Table 8. Summary of laser flash thermal conductivity results for the best candidate discotic LC epoxy films cured with 1,3-propanediamine.

Sample	Density $\rho$ @25°C g/cm <sup>3</sup>	Specific Heat $C_p$ J/g·K	Diffusivity $\alpha$ cm <sup>2</sup> /s	Conductivity $\lambda$ @25°C W/m·K
Epon-828 Epoxy	1.19	1.56	0.00124	0.230
8-arm LC Epoxy (n=4)	1.26	2.27	0.00103	0.30
8-arm LC Epoxy (n=9)	1.07	2.35	0.00097	0.24
Rod-LC Epoxy (DHAMS)	1.27	1.34	0.00176	0.299
Discotic 4arm/8-arm blend	1.39	1.40	0.00141	0.275
Discotic 4arm/aliphatic blend	1.37	1.53	0.00128	0.268

DHAMS was cured with di(4-aminophenyl)disulfone.

### 3.3. Summary of thermal conductivity results for cured discotic LC resins

As can be clearly seen in the results presented in Table 8, the relatively difficult and expensive to synthesize epoxy resins which were the focus of this research project DO NOT enhance thermal conductivity in the z-direction substantially compared to more easily obtainable LC resins (DHAMS), and only moderately better than conventional bis-phenol A epoxy resin. We believe that a more processable version of the DHAMS resin, one that would allow for a much lower curing temperature and higher solubility (via structural modification) will allow for higher thermal conductivity resins to be economically manufactured for composite applications. The metallomesogen based discotic LC epoxy resins developed in this program do not perform as well with respect to mechanical properties of cured films, development of extended molecular order, and economy of manufacture.

### 4. References

- 1) Serrano, J. L. *Metallomesogens: Synthesis, Properties and Applications*; VCH: Weinheim, 1996.
- 2) Stegemeyer, H. *Liquid Crystals*; Steinkopff Darmstadt Springer: New York, 1993.
- 3) Wang, J. "Final Report for United States Air Force Contract F33615-96-5628, Novel Low Cost Thermosets for Advanced Aerospace Composites," Aspen Systems, Inc., 1999.
- 4) Bigg, D. M. *Adv. Polym. Sci.* **1995**, 119, 1.
- 5) Privalko, V. P.; Novikov, V. V. *Adv. Polym. Sci.* **1995**, 119, 33.

- 6)Bigg, D. M. *Polymer Composites* **1986**, *7*, 125.
- 7)Nielsen, L. E. *J. Appl. Polym. Sci.* **1973**, *17*, 3819.
- 8)Agari, Y.; Ueda, A.; Nagai, S. *J. Appl. Polym. Sci.* **1993**, *49*, 1625.
- 9)Proctor, P.; Solc, J. *IEEE Transactions on Components, Hybrids, and Manufacturing Technology* **1991**, *14*, 708.
- 10)Choy, C. L. *Polymer* **1977**, *18*, 984.
- 11)Choy, C. L.; Luk, W. H.; Chen, F. C. *Polymer* **1978**, *19*, 155.
- 12)Chen, F. C.; Choy, C. L.; Young, K. *J. Phys. (D)* **1977**, *10*, 57.
- 13)Achar, B. N.; Fohlen, G. M.; Parker, J. A. *J. Polym. Sci.: Polym. Lett.* **1979**, *17*, 343.
- 14)Achar, B. N.; Fohlen, G. M.; Parker, J. A. *J. Polym. Chem.: Polym. Chem. Ed.* **1983**, *21*.
- 15)Piechocki, C.; Simon, J.; Skoulios, A.; Guillon, D.; Weber, P. *J. Am. Chem. Soc.* **1982**, *104*, 5243.
- 16)van der Pol, J. F.; Neeleman, E.; Zwikker, J. W.; Nolte, R. J. M.; Drenth, W.; Aerts, J.; Visser, R.; Picken, S. *J. Liq. Cryst.* **1989**, *6*, 577.
- 17)Metz, J.; Schneider, O.; Hanack, M. J. M., O. Schneider, M. Hanack, *Inorg. Chem.* **1984**, *23*, 1065.
- 18)Zheng, H.; Lai, C. K.; Swager, T. M. *Chem. Mater.* **1995**, *7*, 2067.
- 19>Ohta, K.; Ema, H.; Muroki, H.; Yamamoto, I. *Mol. Cryst. Liq. Cryst.* **1987**, *147*, 61.